Introduction to Density Functional Theory

Branislav K. Nikolić

Department of Physics and Astronomy, University of Delaware,
Newark, DE 19716, U.S.A.

http://wiki.physics.udel.edu/phys824

Why Study DFT: Reveals Limitations of Simplistic Hamiltonians of Crystalline Materials

TBH with single p_z orbital per C atom and NN hoping

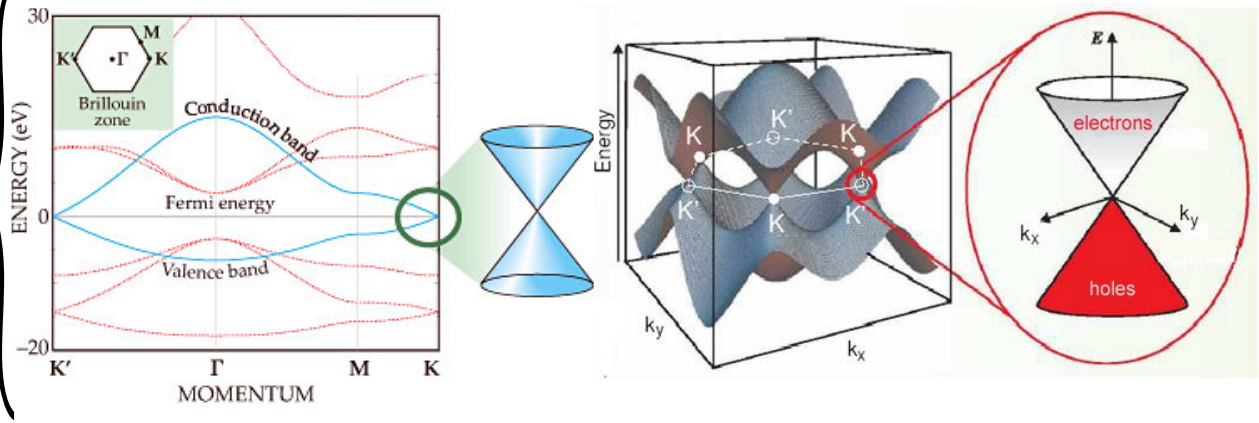

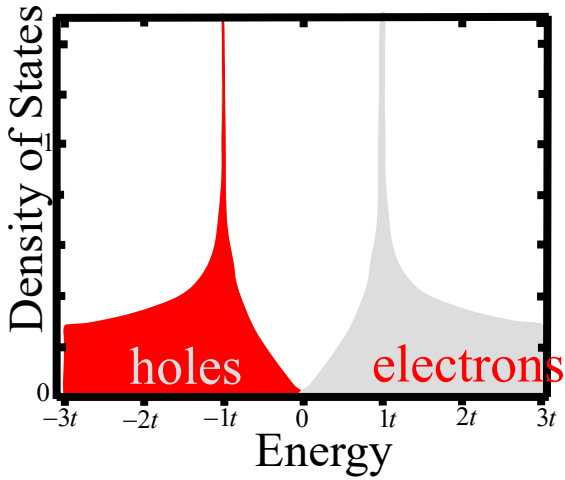

DFT Hamiltonian and its eigenenergies (or "band structure")

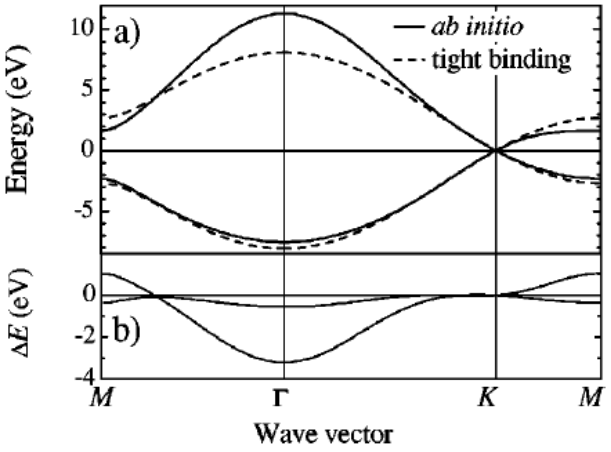

Phys. Rev. **66**, 035412 (2002)

FIG. 2. *Ab initio* and nearest-neighbor tight-binding dispersions of graphene. (a) The converged *ab initio* calculation of the graphene π and π^* electronic bands is shown by the full lines. The dashed lines represent the tight-binding dispersion of Eq. (6) with $s_0=0$ and $\gamma_0=-2.7$ eV. (b) Difference ΔE between the *ab initio* and tight-binding band structures.

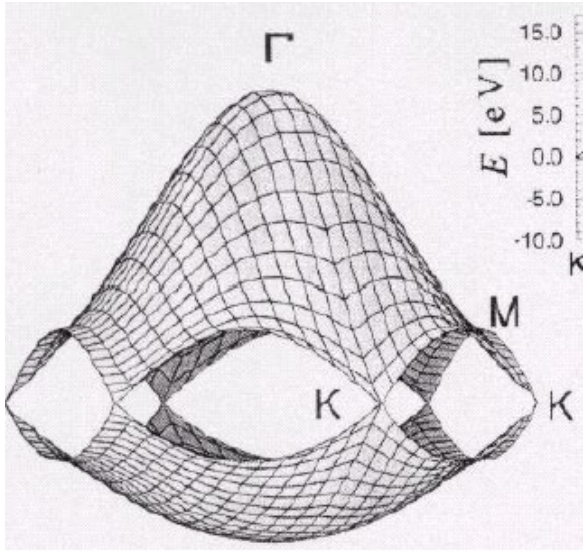

Why Study DFT: Makes Possible Search for New Materials *In Silico*

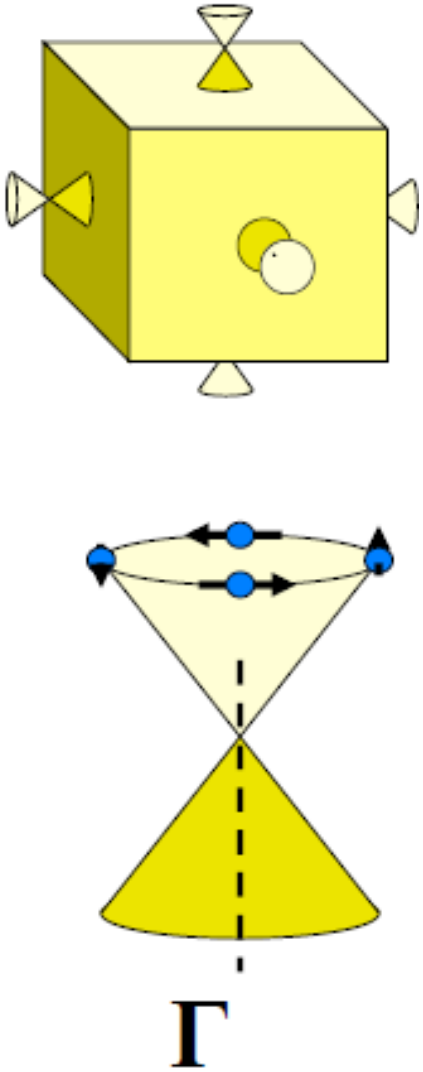

Theory

Topological insulators in Bi_2Se_3, Bi_2Te_3 and Sb_2Te_3 with a single Dirac cone on the surface

Haijun Zhang[1], Chao-Xing Liu[2], Xiao-Liang Qi[3], Xi Dai[1], Zhong Fang[1] and Shou-Cheng Zhang[3]*

DFT calculation

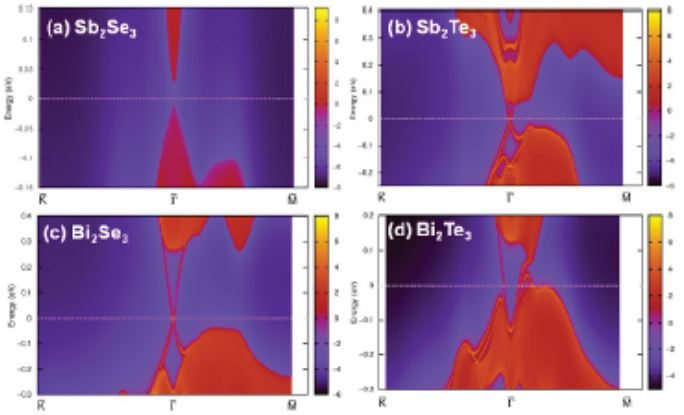

Zhang *et al.*, Nature Physics, 5, 438 (2009)

Experiment

ARPES

Bi_2Se_3

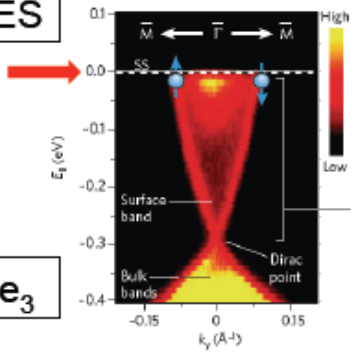

Xia *et al.*, Nature Physics, 5, 398 (2009)

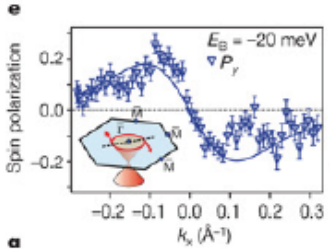

Hsieh, Hasan *et al.*, Nature, 460, 1101 (2009)

Why Study DFT: When Combined with Machine Learning It Allows for High Throughput Search for New Materials

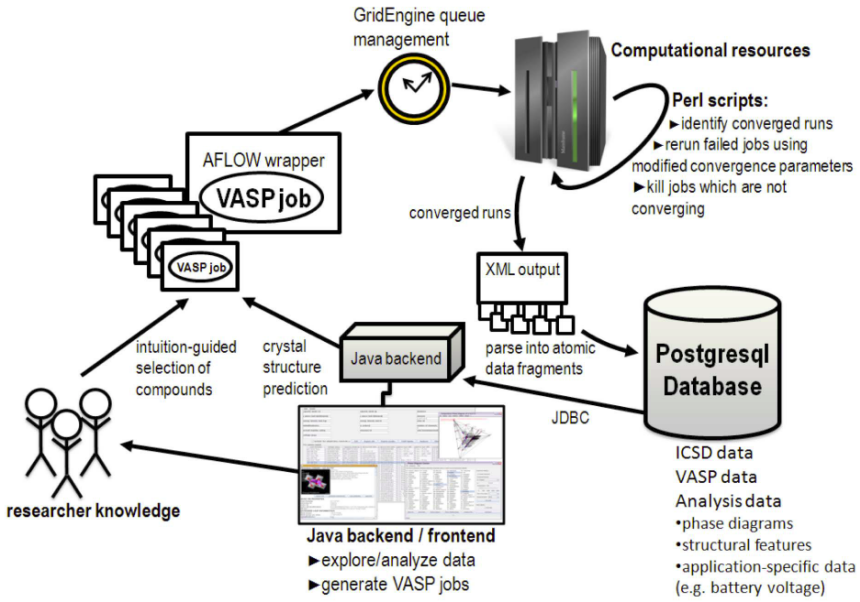

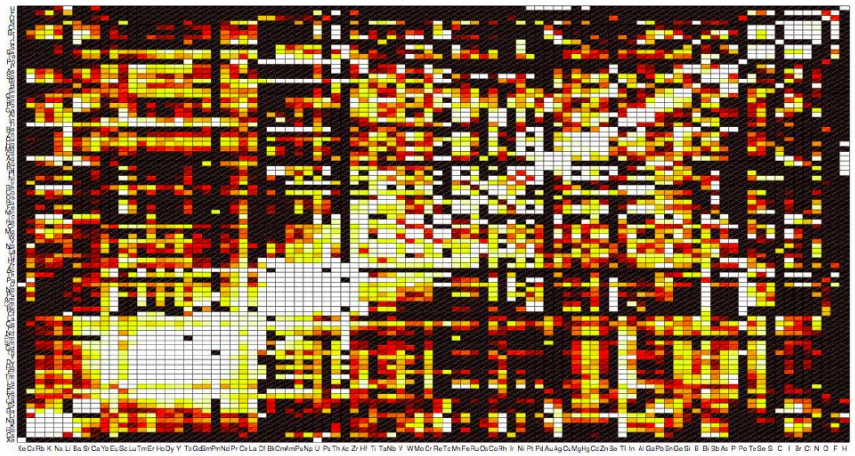

Example: PRL **108**, 068701 (2012) identifies via high-throughput DFT+GW calculations of ~260 generalized $I_pIII_qVI_r$ chalcopyrite materials, out of which 20 are highly efficient for photovoltaic applications (including best known as well as previously unrecognized ones).

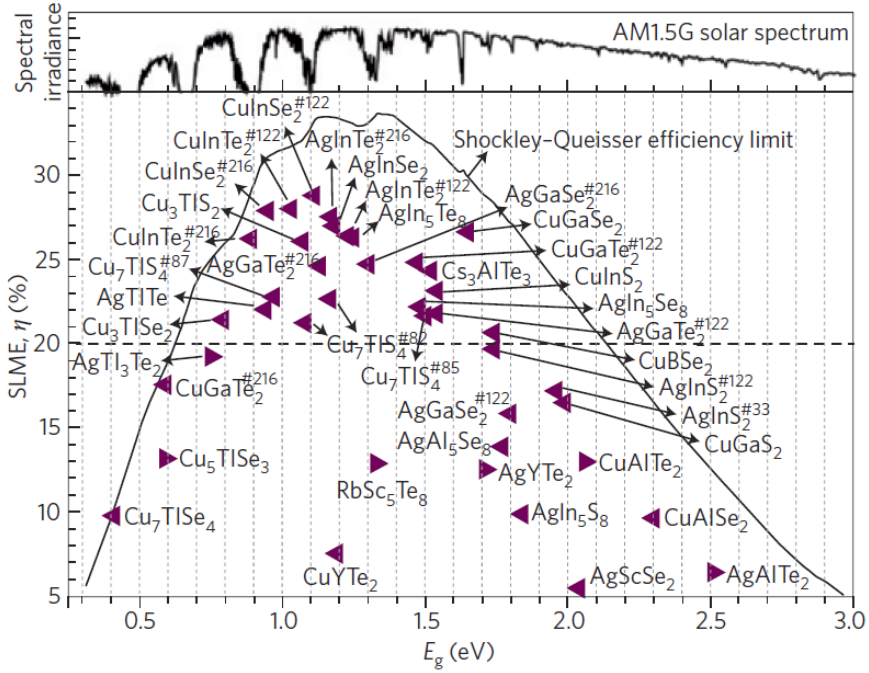

Why Study DFT: Shows the Limitations of Simplistic Hamiltonians of Magnetic Materials

Journal of Magnetism and Magnetic Materials 320 (2008) 1190–1216

Current Perspectives

Spin transfer torques

D.C. Ralph[a,*], M.D. Stiles[b]

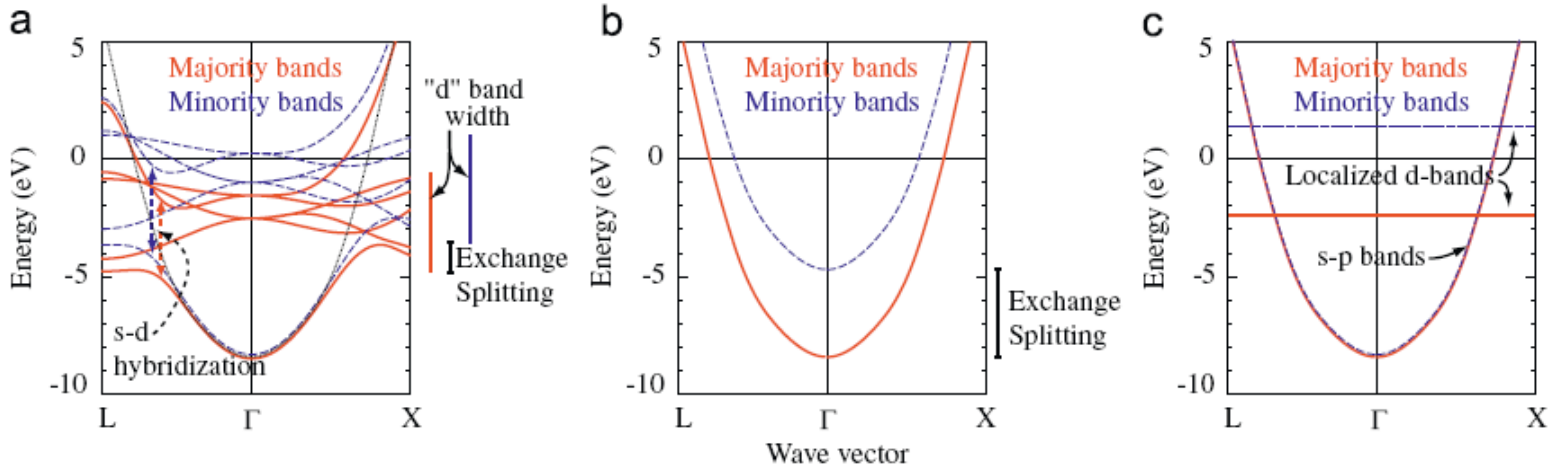

Fig. 4. Model band structures for ferromagnets. The solid red (dashed blue) curves give the majority (minority) bands along two high symmetry directions through the Brillouin zone center, Γ. Panel (a) gives bands calculated in the LSDA for face-centered cubic (fcc) Co. The dotted black curve shows what the energy of the s–p band would be if it were not hybridized with the d bands. The bars to the right of (a) show the width of the d bands and the shift between the majority and minority bands. The dashed arrows in (a) indicated the widths of avoided level-crossings due to the hybridization between the s–p and d bands of the same symmetry along the chosen direction. Panel (b) gives a schematic version of a Stoner model for a ferromagnet. The exchange splitting is larger than in (a) in order to produce a reasonable size moment. The majority and minority Fermi surfaces are more similar to each other than they are for the LSDA model. Panel (c) gives a schematic s–d model band structure. The current-carrying s–p bands have a very small splitting due to the weak exchange interaction with the localized d-states. The majority and minority Fermi surfaces are almost identical.

Why Study DFT: Simplistic Hamiltonians cannot Capture Charge Transfer in Heterostructures

PHYSICAL REVIEW B **90**, 085115 (2014)

Fermi-level pinning, charge transfer, and relaxation of spin-momentum locking at metal contacts to topological insulators

Catalin D. Spataru* and François Léonard
Sandia National Laboratories, Livermore, California 94551, USA
(Received 8 May 2014; revised manuscript received 21 July 2014; published 13 August 2014)

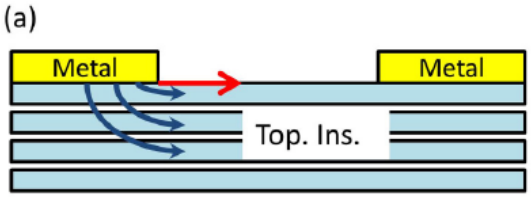

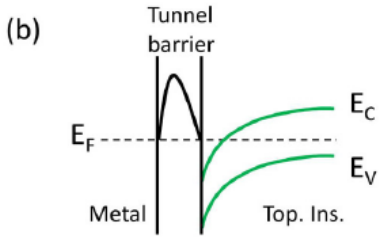

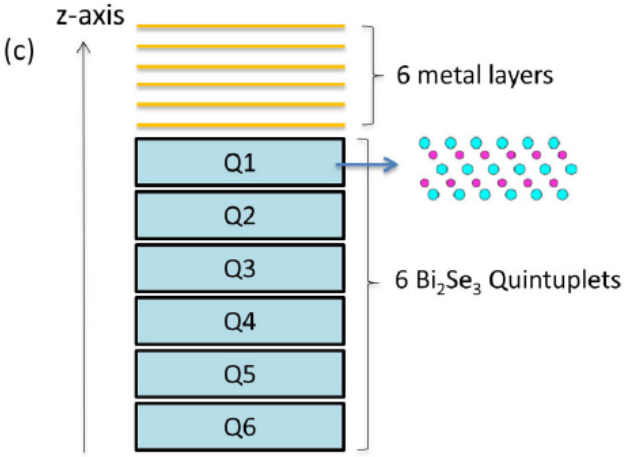

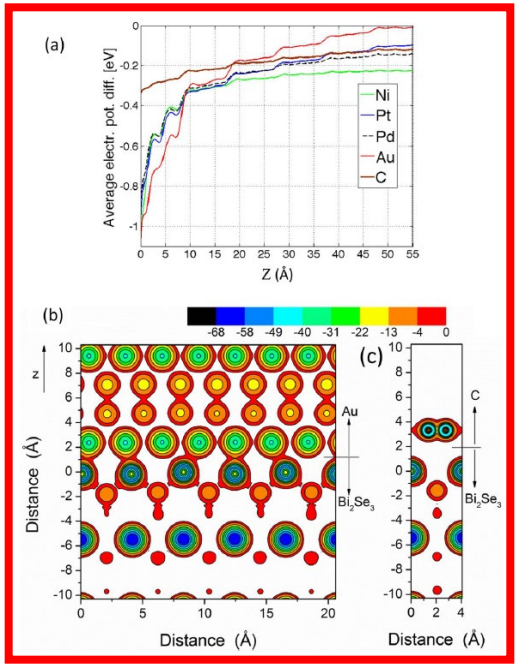

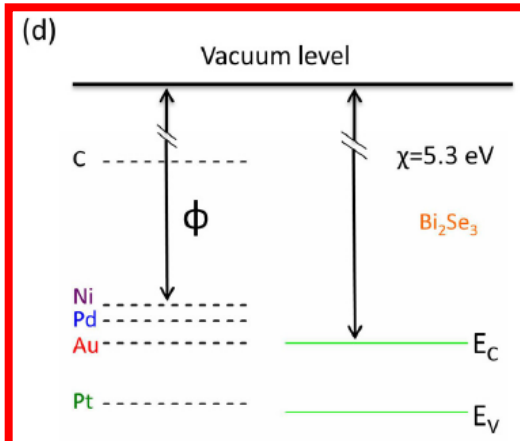

In the simplest picture of the electronic properties of the metal/TI interface, one considers the case of large separation d, such that there is negligible overlap between the TI and metal electron wave functions. In that case the alignment between the metal Fermi level and the TI bands is shown in Fig. 1(d) (before any infinitesimal charge transfer); given the Bi_2Se_3 electron affinity of about 5.3 eV, as well as the bulk band gap of about 0.4 eV, one would expect that Au, Pd, Ni, and graphene would give rise to n-type doping of the TI slab, but that Pt(111) would result in p-type doping. However, our *ab initio* calculations show that for all five contacts the metal Fermi level is located in the conduction band of the TI at the surface.

Why Study DFT: When Combined with Quantum Transport It Can Predict Realistic New Devices

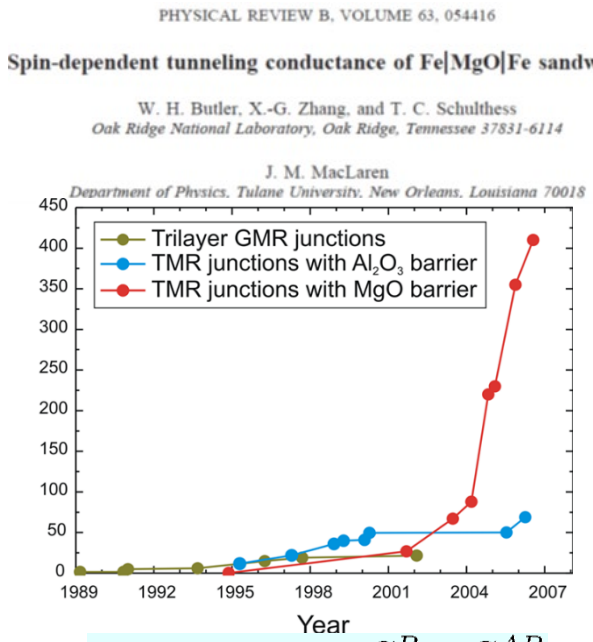

$$\mathrm{TMR}_{\mathrm{optimistic}} = \frac{G^P - G^{AP}}{G^{AP}}$$

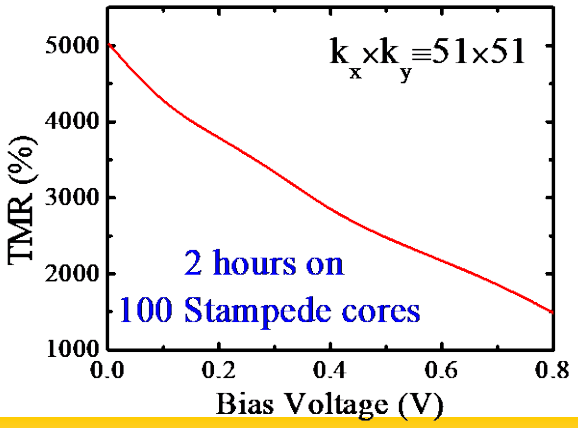

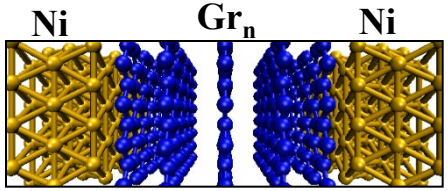

Graphite	a_{hex} = 2.46 Å
Co	a_{hex} = 2.42 Å
Ni	a_{hex} = 2.49 Å
Cu	a_{hex} = 2.57 Å

Ni-Gr mismatch only 1.3%

PRL **99**, 176602 (2007)

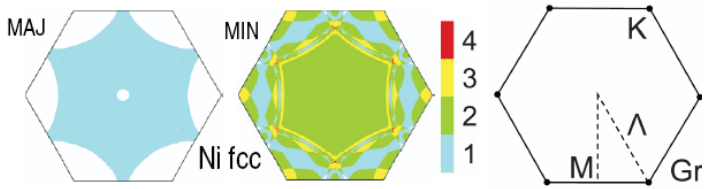

$$\mathrm{TMR}_{\mathrm{pesimistic}} = \frac{G^P - G^{AP}}{G^P + G^{AP}}$$

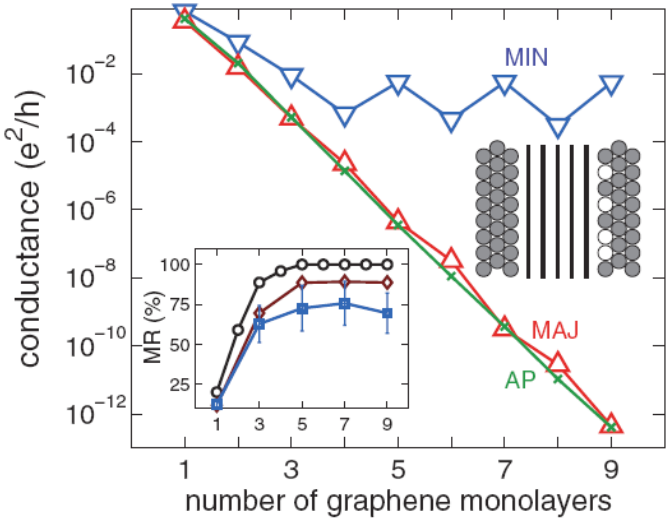

PRB **85**, 184426 (2012)

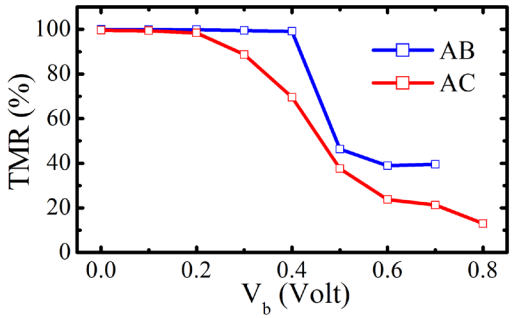

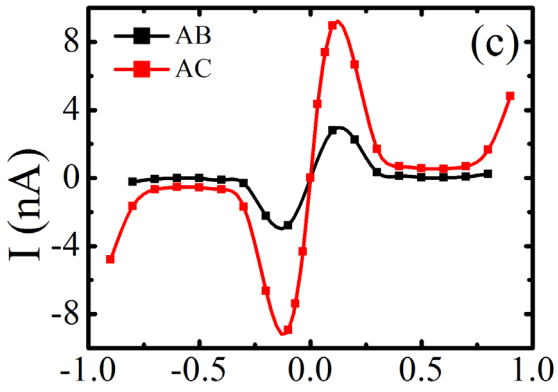

Quantum-Mechanical Many-Body Problem for Electrons in Solids

- Hamiltonian of electrons in solid after Born-Oppenheimer approximation:

$$\hat{H} = \sum_i \left[-\frac{\hbar^2 \Delta_i}{2m_e} + \sum_l \frac{-e^2}{4\pi\epsilon_0} \frac{Z_l}{|\mathbf{r}_i - \mathbf{R}_l|} \right] + \frac{1}{2} \sum_{i \neq j} \frac{e^2}{4\pi\epsilon_0} \frac{1}{|\mathbf{r}_i - \mathbf{r}_j|}.$$

To calculate material properties, one has to take into account three terms: The kinetic energy favoring the electrons to move through the crystal (blue), the lattice potential of the ions (green), and the Coulomb interaction between the electrons (red). Due to the latter, the first electron is repelled by the second, and it is energetically favorable to hop somewhere else, as depicted. **Hence, the movement of every electron is correlated with that of every other, which prevents even a numerical solution.**

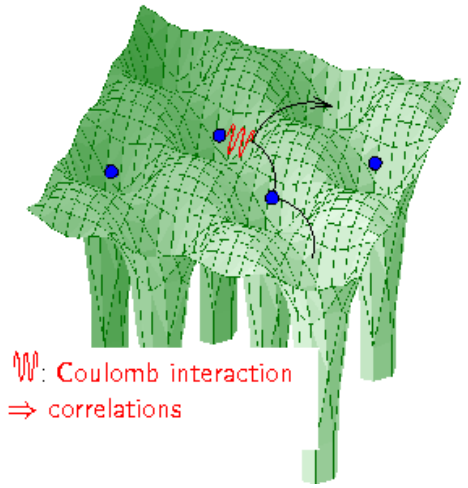

- Many traditional approaches to solving difficult many-body problem begin with the Hartree-Fock approximation, in which many-particle wavefunction is approximated by a single Slater determinant of orbitals (single-particle wavefunctions) and the energy is minimized. **These include configuration interaction, coupled cluster, and Møller-Plesset perturbation theory, and are mostly used for finite systems, such as molecules in the gas phase.** Other approaches use reduced descriptions, such as the density matrix or Green function, but leading to an infinite set of coupled equations that must somehow be truncated.

Density Functional Theory Approach to Quantum Many-Body Problem

- Conventional quantum-mechanical approach to many-body systems:

$$v(\mathbf{r}) \overset{SE}{\Longrightarrow} \Psi(\mathbf{r}_1, \mathbf{r}_2 \ldots, \mathbf{r}_N) \overset{\langle\Psi|\ldots|\Psi\rangle}{\Longrightarrow} \text{observables}$$

$$E_{v,0} = E_v[\Psi_0] = \langle\Psi_0|\hat{H}|\Psi_0\rangle \leq \langle\Psi'|\hat{H}|\Psi'\rangle = E_v[\Psi']$$

$$n(\mathbf{r}) = N \int d^3r_2 \int d^3r_3 \ldots \int d^3r_N \Psi^*(\mathbf{r}, \mathbf{r}_2 \ldots, \mathbf{r}_N)\Psi(\mathbf{r}, \mathbf{r}_2 \ldots, \mathbf{r}_N)$$

- DFT conceptual structure:

$$n(\mathbf{r}) \Longrightarrow \Psi(\mathbf{r}_1, \ldots, \mathbf{r}_N) \Longrightarrow v(\mathbf{r})$$

Knowledge of electron density implies knowledge of the wave function and the potential, and hence of all other observables. Although this sequence describes the conceptual structure of DFT, it does not really represent what is done in actual applications of it, which typically proceed along rather different lines, and do not make explicit use of many-body wave functions

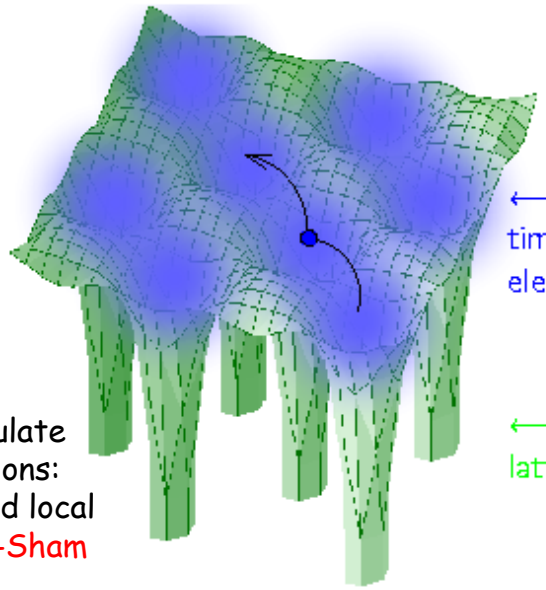

- DFT in computational practice:

Local Density Approximation (LDA) is an approximation which allows to calculate material properties but which dramatically simplifies the electronic correlations: Every electron moves independently, i.e., uncorrelated, within a time-averaged local density of the other electrons, as described by a set of single-particle Kohn-Sham equations whose solutions ("orbitals") are used the built the density.

Computational Complexity: Many-Body Wave Function vs. Electron Density vs. KS Orbitals

A Bird's-Eye View of Density-Functional Theory

Klaus Capelle

Departamento de Física e Informática
Instituto de Física de São Carlos
Universidade de São Paulo
Caixa Postal 369, São Carlos, 13560-970 SP, Brazil

[6]A simple estimate of the computational complexity of this task is to imagine a real-space representation of Ψ on a mesh, in which each coordinate is discretized by using 20 mesh points (which is not very much). For N electrons, Ψ becomes a function of $3N$ coordinates (ignoring spin, and taking Ψ to be real), and 20^{3N} values are required to describe Ψ on the mesh. The density $n(\mathbf{r})$ is a function of three coordinates, and requires 20^3 values on the same mesh. CI and the Kohn-Sham formulation of DFT additionally employ sets of single-particle orbitals. N such orbitals, used to build the density, require $20^3 N$ values on the same mesh. (A CI calculation employs also unoccupied orbitals, and requires more values.) For $N = 10$ electrons, the many-body wave function thus requires $20^{30}/20^3 \approx 10^{35}$ times more storage space than the density, and $20^{30}/(10 \times 20^3) \approx 10^{34}$ times more than sets of single-particle orbitals. Clever use of symmetries can reduce these ratios, but the full many-body wave function remains unaccessible for real systems with more than a few electrons.

DFT is Based on the Exact Hohenberg-Kohn Theorem

1. The nondegenerate ground-state (GS) wave function is a unique functional of the GS density:

$$\Psi_0(\mathbf{r}_1, \mathbf{r}_2 \ldots, \mathbf{r}_N) = \Psi[n_0(\mathbf{r})]$$

2. The GS energy, as the most important observable, has variational property:

$$E_{v,0} = E_v[n_0] = \langle \Psi[n_0] | \hat{H} | \Psi[n_0] \rangle \qquad E_v[n_0] \leq E_v[n']$$

3. Kinetic energy and electron-electron interaction energy are universal (system independent) functionals of electron density:

$$E_v[n] = T[n] + U[n] + V[n] = F[n] + V[n]$$

while non-universal potential energy in external field is obtained from:

$$V[n] = \int d^3r \, n(\mathbf{r}) v(\mathbf{r})$$

4. If external potential $v(\mathbf{r})$ is not held fixed, the functional $V[n]$ becomes universal: the GS density determines not only the GS wave function Ψ_0, but, up to an additive constant, also the potential $V[n_0]$. **CONSEQUENCE:**

$$E_0 = E[n_0] = \langle \Psi[n_0] | \hat{T} + \hat{U} + \hat{V}[n_0] | \Psi[n_0] \rangle \qquad \Psi_k(\mathbf{r}_1, \mathbf{r}_2 \ldots, \mathbf{r}_N) = \Psi_k[n_0]$$

Two Step Formal Construction of the Energy Density Functional

$$E[n] = \min \left\{ \langle \Psi | \hat{H} | \Psi \rangle \;\middle|\; \langle \Psi | \sum_{i=1}^{N} \delta(\mathbf{r} - \mathbf{r_i}) | \Psi \rangle = n(\mathbf{r}) \right\}$$

$$E_0 = \min_n E[n]$$

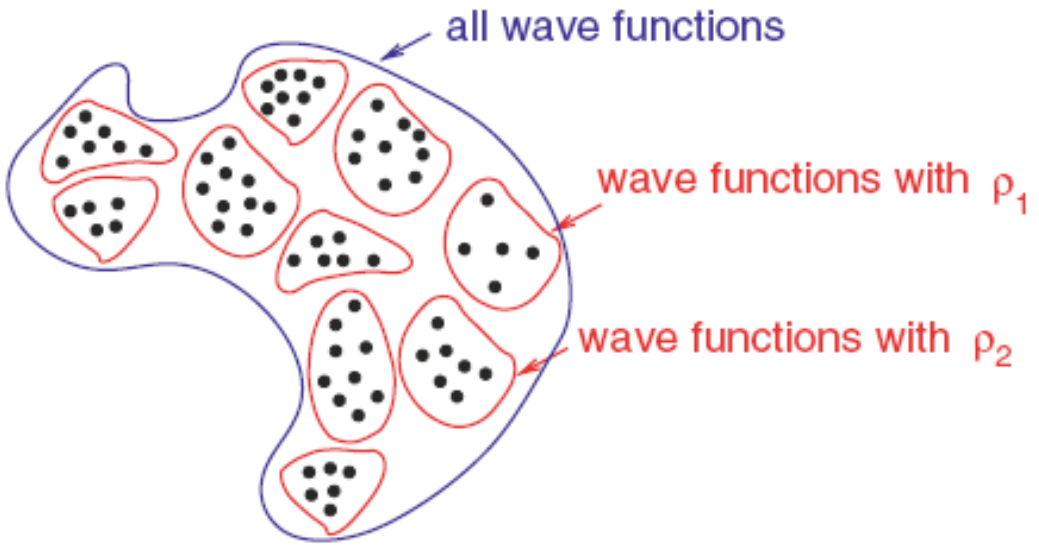

- While this construction proves the Hohenberg-Kohn theorem, we did not actually gain anything: to obtain the functional $E[n]$ we have to calculate the expectation value $\langle \Psi | \hat{H} | \Psi \rangle$ for complicated many-body wave functions $\Psi(\mathbf{r}_1\sigma_1, \ldots \mathbf{r}_N\sigma_N)$.

Functionals and Functional Derivatives

- Function vs. Functional:

$x \mapsto f(x)$ function maps number to a number

$n(\mathbf{r}) \mapsto F[n]$ functional maps whole function to a number; example: $N = \int d^3\mathbf{r}\, n(\mathbf{r}) = N[n]$

$F[n(\mathbf{r})]$ is the same as $F[n(\mathbf{r}')]$

- Standard Derivative vs. Functional Derivative:

$$f(x+dx) = f(x) + \frac{df}{dx}dx + O(dx^2)$$

$$F[f(x)+\delta f(x)] = F[f(x)] + \int dx\, \frac{\delta F[f]}{\delta f(x)}\delta f(x) + O(\delta f^2)$$

the integral arises because the variation in the functional F is determined by variations in the function at all points in space

- Useful formula:

$$F[n] = \int f(n, n', n'', n''', ...; x)dx \Rightarrow \frac{\delta F[n]}{\delta n(x)} = \frac{\partial f}{\partial n} - \frac{d}{dx}\frac{\partial f}{\partial n'} + \frac{d^2}{dx^2}\frac{\partial f}{\partial n''} - \frac{d^3}{dx^3}\frac{\partial f}{\partial n'''} + ...$$

Example from classical mechanics:

$$\mathcal{A}[q] = \int \mathcal{L}(q, \dot{q}; t)dt \Rightarrow 0 = \frac{\delta \mathcal{A}[q]}{\delta q(t)} = \frac{\partial \mathcal{L}}{\partial q} - \frac{d}{dt}\frac{\partial \mathcal{L}}{\partial \dot{q}}$$

Practical DFT: Kohn-Sham Equations

- Only the ionic (external for electrons) and the Hartree (i.e., classical Coulomb) potential energy can be expressed easily through the electron density:

$$E_{\rm ion}[n] = \int d^3\mathbf{r}\; V_{\rm ion}(\mathbf{r})\; n(\mathbf{r}) \qquad E_{\rm Hartree}[n] = \frac{1}{2}\int d^3\mathbf{r}'\, d^3\mathbf{r}\; V_{\rm ee}(\mathbf{r}-\mathbf{r}')\; n(\mathbf{r}')n(\mathbf{r})$$

- Using the kinetic energy functional, all of the difficulty of electron-electron interactions is absorbed into the exchange-correlation term:

$$E[n] = E_{\rm kin}[n] + E_{\rm ion}[n] + E_{\rm Hartree}[n] + E_{\rm xc}[n]$$

Although the exact form of $E_{\rm xc}[n]$ is unknown, an important aspect of DFT is that the functional $E[n] - E_{\rm ion}[n]$ does not depend on the material investigated, so that if we knew the DFT functional for one material, we could calculate all materials by simply adding $E_{\rm ion}[n]$.

- To calculate the ground-state energy and density, we have to minimize:

$$\frac{\delta}{\delta n(\mathbf{r})}\left\{E[n] - \lambda\left(\int d^3\mathbf{r}\rho(\mathbf{r}) - N\right)\right\} = 0 \overset{\rm Kohn-Sham}{\Longrightarrow} \frac{\delta}{\delta\varphi_i(\mathbf{r})}\left\{E[n] - \varepsilon_i\left[\int d^3\mathbf{r}|\varphi_i(\mathbf{r})|^2\right] - 1\right\} = 0$$

$$n(\mathbf{r}) = \sum_{i=1}^{N}|\varphi_i(\mathbf{r})|^2$$

Kohn-Sham: Electron density expressed in terms of auxiliary one-particle wave function

$$\left[-\frac{\hbar^2}{2m_e}\Delta + V_{\rm ion}(\mathbf{r}) + \int d^3\mathbf{r}'\; V_{\rm ee}(\mathbf{r}-\mathbf{r}')n(\mathbf{r}') + \frac{\delta E_{\rm xc}[n]}{\delta n(\mathbf{r})}\right]\varphi_i(\mathbf{r}) = \varepsilon_i\;\varphi_i(\mathbf{r})$$

Kohn-Sham: The final result is a set of one-particle Schrödinger equations describing single electrons moving in time-averaged potential of all electrons

Kohn-Sham Equations in the Local Density Approximation (LDA)

- The one-particle Kohn-Sham equations, in principle, only serve the purpose of minimizing the DFT energy, and have no physical meaning.

- If we knew the exact $E_{\rm xc}[n]$, which is non-local in $n(\mathbf{r})$, we would obtain the exact ground state energy and density. In practice, one has to make approximations to $E_{\rm xc}[n]$ such as the LDA:

$$E_{\rm xc}[n] \overset{\rm LDA}{\approx} \int d^3\mathbf{r}\; E_{\rm xc}^{\rm LDA}(n(\mathbf{r}))$$

$E_{\rm xc}^{\rm LDA}[n(\mathbf{r})]$ is typically calculated from the perturbative solution or the numerical simulation of the jellium model which is defined by $V_{\rm ion}(\mathbf{r}) = {\rm const}$. Owing to translational symmetry, the jellium model has a constant electron density $n(\mathbf{r}) = n_0$. Hence, with the correct jellium $E_{\rm xc}^{\rm LDA}[n(\mathbf{r})]$, we could calculate the energy of any material with a constant electron density exactly. **However, for real materials $n(\mathbf{r})$ is varying, less so for s and p valence electrons but strongly for d and f electrons.**

NOTE: The kinetic energy in KS equations is that of independent (uncorrelated) electrons. The true kinetic energy functional for the many-body problem is different. We hence have to add the difference between the true kinetic energy functional for the many-body problem and the above uncorrelated kinetic energy to $E_{\rm xc}$, **so that all many-body difficulties are buried in $E_{\rm xc}$.**

$$E_{\rm kin}[n_{\rm min}] = -\sum_{i=1}^{N} \langle \varphi_i | \hbar^2 \Delta/(2m_e) | \varphi_i \rangle$$

Kohn-Sham Quasiparticle "Drags" Exchange-Correlation Hole Surrounding Bare Electron

Wave function of two non-interacting electrons

$$\Psi_{ij} = \frac{1}{\sqrt{2}V}\left(e^{i\mathbf{k}_i\cdot\mathbf{r}_i}e^{i\mathbf{k}_j\cdot\mathbf{r}_j} - e^{i\mathbf{k}_i\cdot\mathbf{r}_j}e^{i\mathbf{k}_j\cdot\mathbf{r}_i}\right) = \frac{1}{\sqrt{2}V}e^{i(\mathbf{k}_i\cdot\mathbf{r}_i+\mathbf{k}_j\cdot\mathbf{r}_j)}\left(1 - e^{-i(\mathbf{k}_i-\mathbf{k}_j)\cdot(\mathbf{r}_i-\mathbf{r}_j)}\right)$$

$$|\Psi_{ij}|^2 d\mathbf{r}_i d\mathbf{r}_j = \frac{1}{V^2}[1-\cos(\mathbf{k}_i-\mathbf{k}_j)\cdot(\mathbf{r}_i-\mathbf{r}_j)]d\mathbf{r}_i d\mathbf{r}_j$$

Probability to find electron i in some small volume dr_i while electron j is in some small volume dr_j

$$P(r)_{\uparrow\uparrow}d\mathbf{r} = n_\uparrow[1-\cos(\mathbf{k}_i-\mathbf{k}_j)\cdot\mathbf{r}]_{\text{aver over FS}} \Leftrightarrow n_{\text{ex}}(\mathbf{r}) = en/2[1-\cos(\mathbf{k}_i-\mathbf{k}_j)\cdot\mathbf{r}]_{\text{aver over FS}}$$

$$n_{\text{eff}}(\mathbf{r}) = en/2 + n_{\text{ex}}(\mathbf{r}) = en\left[1 - \frac{9}{2}\frac{(\sin k_F r - k_F r\cos k_F r)^2}{(k_F r)^6}\right]$$

Effective charge density seen by an electron of a given spin orientation in a non-interacting electron gas

PHYSICAL REVIEW B **69**, 233105 (2004)

Spin-resolved pair-distribution functions in an electron gas: A scattering approach based on consistent potentials

I. Nagy,[1,2] R. Díez Muiño,[2,3] J. I. Juaristi,[3,4] and P. M. Echenique[2,3,4]

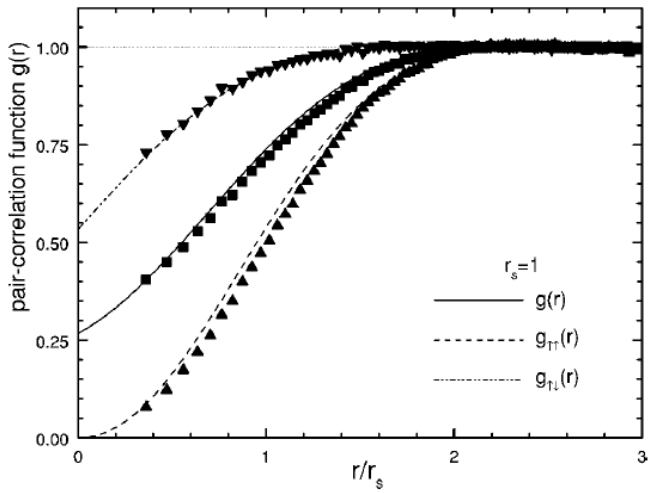

VOLUME 87, NUMBER 3 PHYSICAL REVIEW LETTERS 16 JULY 2001

Quantum Monte Carlo Analysis of Exchange and Correlation in the Strongly Inhomogeneous Electron Gas

Maziar Nekovee,[1,*] W. M. C. Foulkes,[1] and R. J. Needs[2]

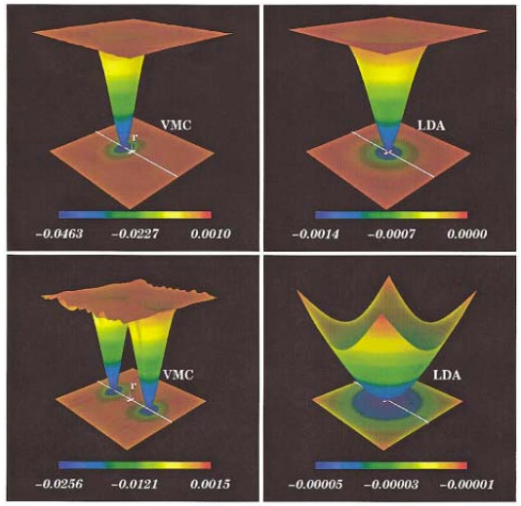

Practical DFT: Pseudopotentials

- If we knew the DFT functional for one material, we could treat all materials by simply adding ionic potentic which is typically approximated by pseudopotentials

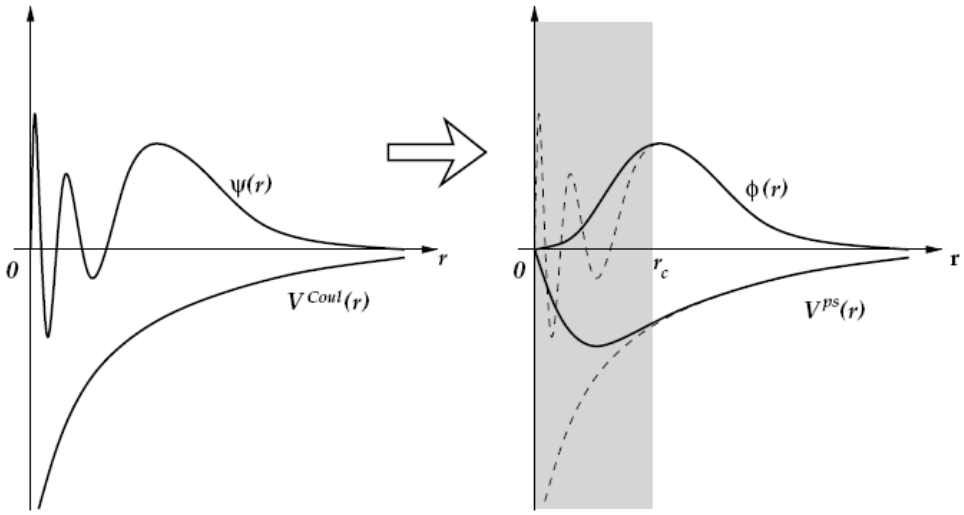

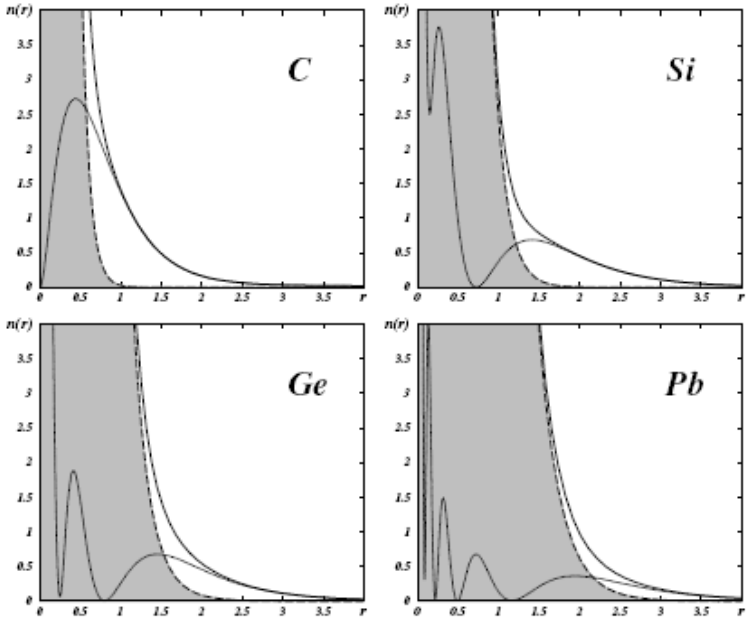

Figure 2.4. Electron densities $n(r)$ as a function of the radial distance from the nucleus r in angstroms, for four elements of column IV of the Periodic Table: C ($Z = 6$, $[1s^2]2s^22p^2$), Si ($Z = 14$, $[1s^22s^22p^6]3s^23p^2$), Ge ($Z = 32$, $[1s^22s^22p^63s^23p^63d^{10}]4s^24p^2$) and Pb ($Z = 82$, $[1s^22s^22p^63s^23p^63d^{10}4s^24p^64d^{10}4f^{14}5s^25p^65d^{10}]6s^26p^2$); the core states are given inside square brackets. In each case, the dashed line with the shaded area underneath it represents the density of core electrons, while the solid line represents the density of valence electrons and the total density of electrons (core plus valence). The core electron density for C is confined approximately below 1.0 Å, for Si below 1.5 Å, for Ge below 2.0 Å, and for Pb below 2.5 Å. In all cases the valence electron density extends well beyond the range of the core electron density and is relatively small within the core. The wiggles that develop in the valence electron densities for Si, Ge and Pb are due to the nodes of the corresponding wavefunctions, which acquire oscillations in order to become orthogonal to core states.

Solve $H^{sp}\psi^{(v)}(r) = [\hat{F} + V^{Coul}(r)]\psi^{(v)}(r) = \epsilon^{(v)}\psi^{(v)}(r)$

↓

Fix pseudo-wavefunction $\phi^{(v)}(r) = \psi^{(v)}(r)$ for $r \geq r_c$

↓

Construct $\phi^{(v)}(r)$ for $0 \leq r < r_c$, under the following conditions:

$\phi^{(v)}(r)$ smooth, nodeless; $d\phi^{(v)}/dr$, $d^2\phi^{(v)}/dr^2$ continuous at r_c

↓

Normalize pseudo-wavefunction $\phi^{(v)}(r)$ for $0 \leq r < \infty$

↓

Invert $[\hat{F} + V^{ps}(r)]\phi^{(v)}(r) = \epsilon^{(v)}\phi^{(v)}(r)$

↓

$V^{ps}(r) = \epsilon^{(v)} - [\hat{F}\phi^{(v)}(r)]/\phi^{(v)}(r)]$

E. Kaxiras, *Atomic and electronic structure of solids* (CUP, 2003)

Solving Kohn-Sham Equations via Self-Consistent Loop of Software Packages

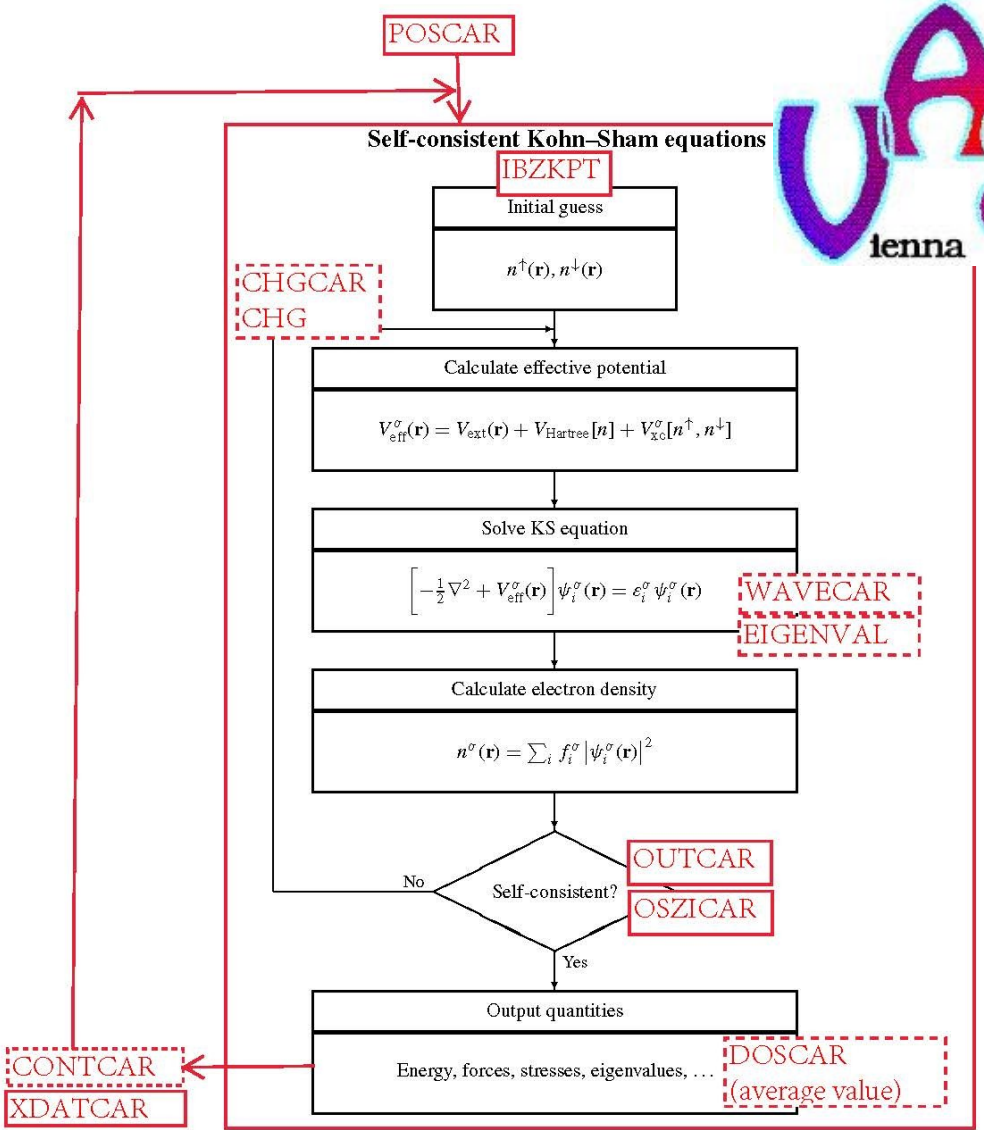

b-initio VASP Package Vienna Simulation

QUANTUM ESPRESSO

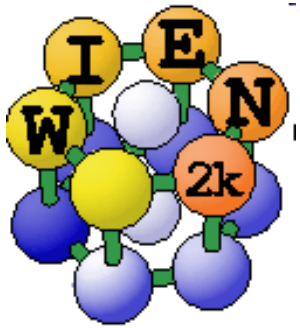

www.flapw.de

fleur

GPAW!

abinit.org

Welcome to OpenMX

Open source package for Material eXplorer

Add information

update information

siesta A linear-scaling density-functional method

Home | The Siesta Project | Licenses | Docu

Examples: DFT Applied to Quantum Chemistry and thereby Inspired Hybrid Functionals

http://dft.uci.edu/dftbook.html

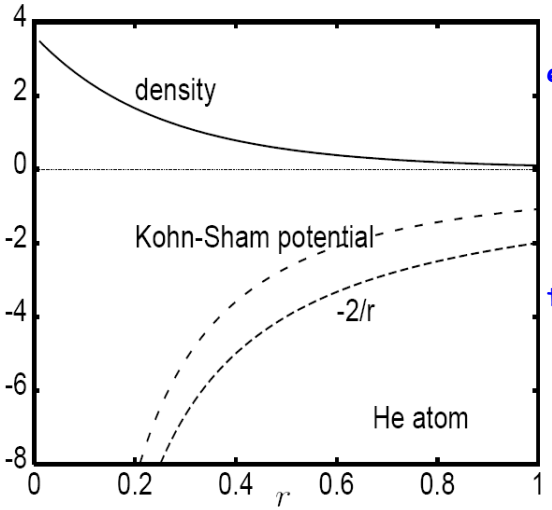

Two non-interacting **Kohn-Sham electrons** (doubly occupying 1s orbital) in this potential have precisely the same density as the interacting electrons in **He atom** → if we can figure out some way to approximate this potential accurately, we have a much less demanding set of equations to solve than those of the true system

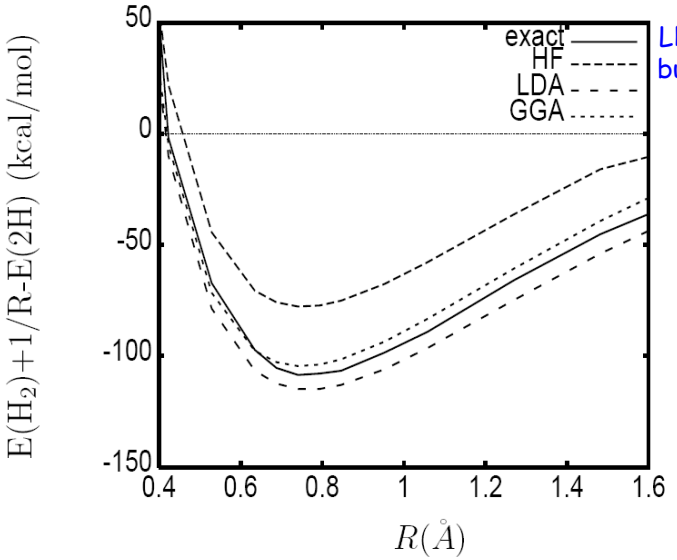

LDA greatly improves on Hartree-Fock, but it typically overbinds by about 1 eV, which is too inaccurate for quantum chemistry, but sufficient for many solid-state calculations

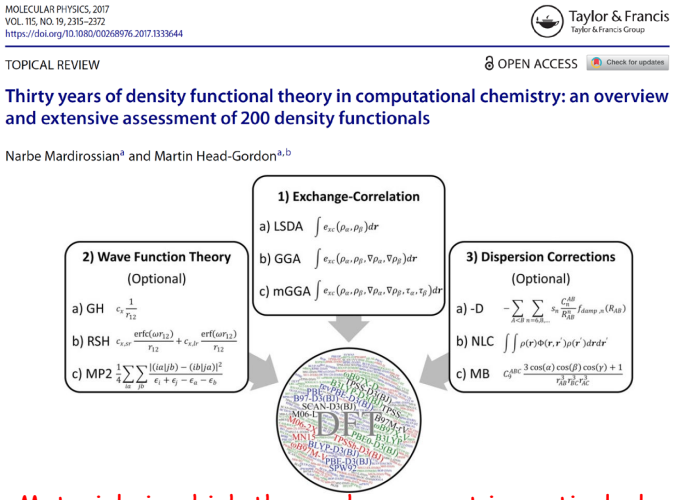

Materials in which the exchange part is particularly important are, e.g., semiconductors. Here, DFT within LDA or GGA predicts consistently too small band gaps. This can be overcome by hybrid functionals that mix part of the exact exchange to the exchange correlation functional. The amount of exact exchange that is required for an accurate modeling is, however, non-universal, i.e., material-dependent

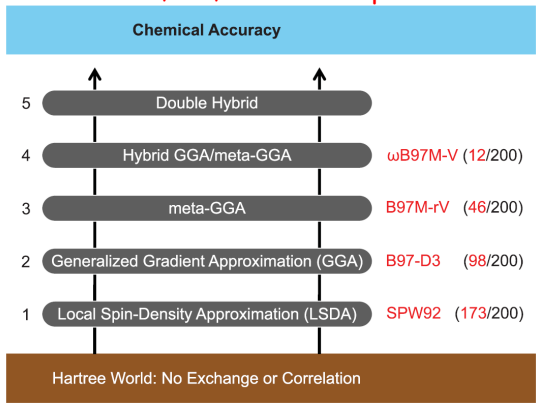

DFT+GW Fitted with Slater-Koster TBH using p_z, d_{yz}, d_{zx} Orbitals per C Atom

JOURNAL OF APPLIED PHYSICS **109**, 104304 (2011)

Accurate six-band nearest-neighbor tight-binding model for the π-bands of bulk graphene and graphene nanoribbons

Timothy B. Boykin,[1,a] Mathieu Luisier,[2] Gerhard Klimeck,[2] Xueping Jiang,[3] Neerav Kharche,[3] Yu Zhou,[3] and Saroj K. Nayak[3]

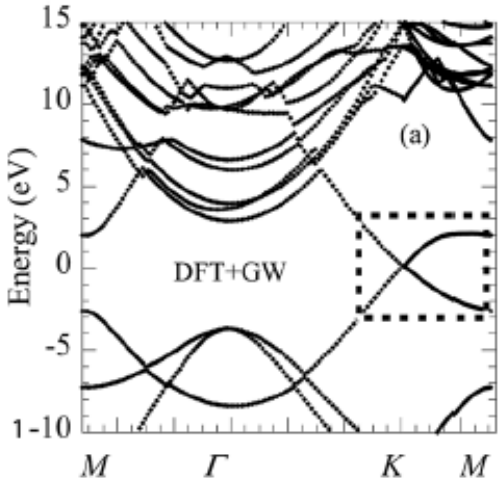

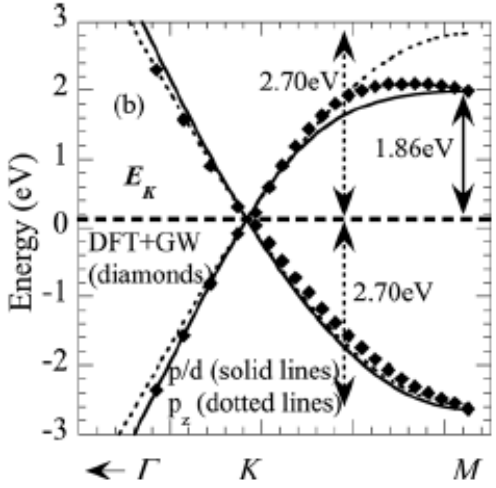

Slater-Koster hopping parameters (in eV)

C-C		H-C	
$E_p(C)$	1.2057	$E_p(H)$	13.04020
$E_d(C)$	24.1657	$E_d(H)$	20.9020
$pp\pi$	−3.2600	$pp\pi$	−0.61754
$pd\pi$	2.4000	$pd\pi$	3.41170
$dd\pi$	3.6000	$dd\pi$	10.44660
$dd\delta$	−7.4000	$dd\delta$	−13.96340

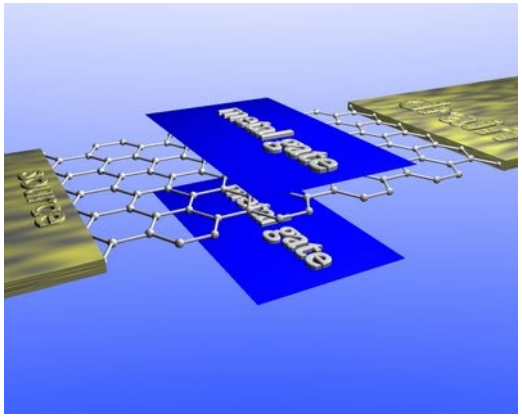

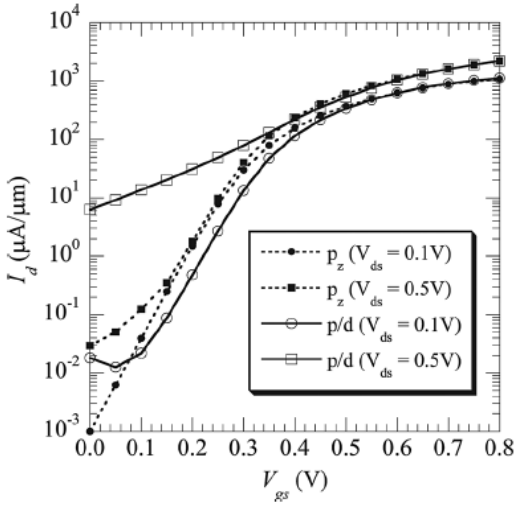

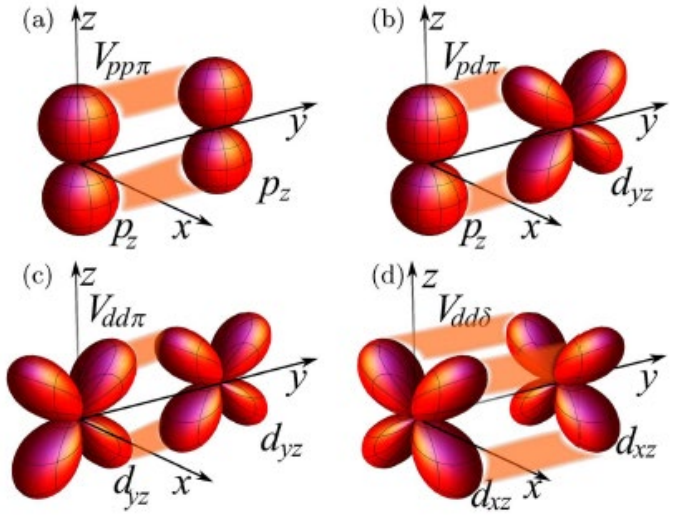

Alternative *Ab Initio* TBH for Graphene with Single p_z Orbital per C Atom and 3NN Hoppings

PHYSICAL REVIEW B **66**, 035412 (2002)

Tight-binding description of graphene

S. Reich, J. Maultzsch, and C. Thomsen
Institut für Festkörperphysik, Technische Universität Berlin, Hardenbergstrasse 36, 10623 Berlin, Germany

P. Ordejón
Institut de Ciència de Materials de Barcelona (CSIC), Campus de la U.A.B. E-08193 Bellaterra, Barcelona, Spain

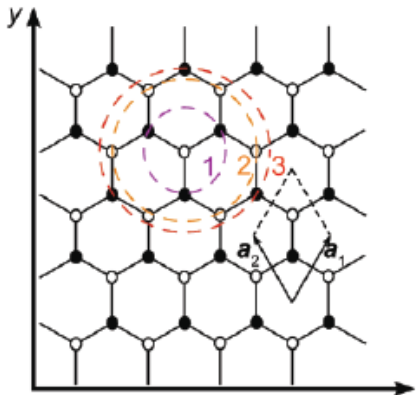

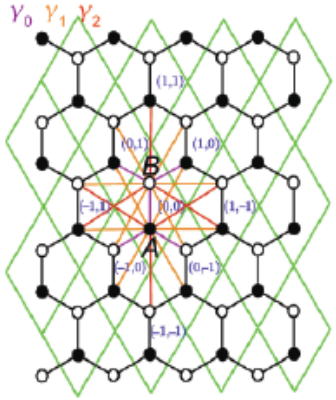

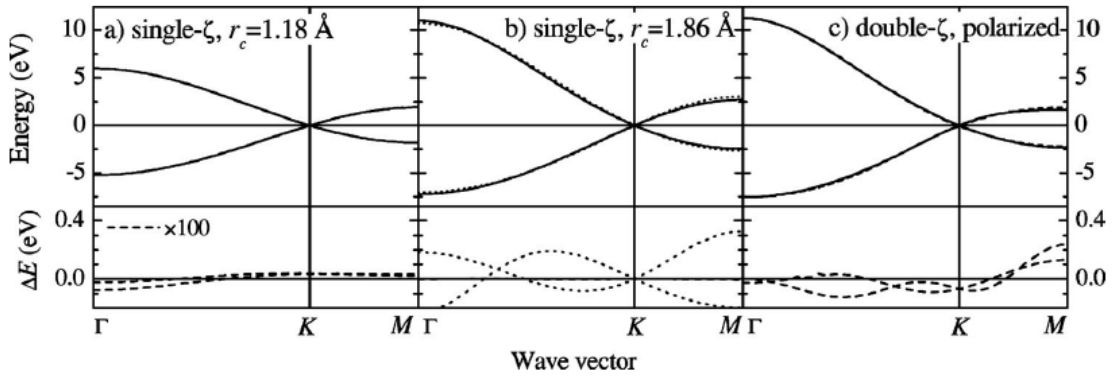

FIG. 3. (a) Top: first-principles band structure with a single-ζ basis set and $r_c = 1.18$ Å. The nearest-neighbor tight-binding band structure [Eq. (6)] with $\gamma_0 = -1.86$ eV and $s_0 = 0.02$ coincides with the first-principles result. Bottom: difference ΔE between the first-principles and nearest-neighbor tight-binding band structures. (b) Top, full lines: first-principles result with a single-ζ basis set and $r_c = 1.86$ Å; dotted lines: nearest-neighbor tight-binding band structure [Eq. (6)] with $\gamma_0 = -2.84$ eV and $s_0 = 0.070$; the third-nearest neighbor tight-binding band structure coincides with the first-principles result shown by the full lines ($\varepsilon_{2p} = -0.36$ eV, $\gamma_0 = -2.78$ eV, $\gamma_1 = -0.12$ eV, $\gamma_2 = -0.068$ eV, $s_0 = 0.106$, $s_1 = 0.001$, and $s_2 = 0.003$). Bottom, dotted line: difference between the first-principles and the nearest-neighbor tight-binding band structure shown in the top panel. For the third-nearest neighbor tight-binding approximation the differences are not seen on the chosen energy scale. (c) Top: converged *ab initio* (full lines) and third-neighbor tight-binding (dashed) band structures; see Table I for the tight-binding parameters ($M\Gamma KM$). Bottom: difference between the two band structures above.

DFT fitted with Slater-Koster TBH for Monolayer MoS_2

IOP Publishing
J. Phys.: Condens. Matter **27** (2015) 365501 (21pp)
Journal of Physics: Condensed Matter
doi:10.1088/0953-8984/27/36/365501

A tight-binding model for MoS_2 monolayers

E Ridolfi[1], D Le[2], T S Rahman[2], E R Mucciolo[2] and C H Lewenkopf[1]

[1] Instituto de Física, Universidade Federal Fluminense, 24210-346 Niterói, RJ, Brazil
[2] Department of Physics, University of Central Florida, Orlando, FL 32816-2385, USA

E-mail: emilia.ridolfi@gmail.com, mucciolo@physics.ucf.edu and caio@if.uff.br

Received 2 July 2015, revised 16 July 2015
Accepted for publication 22 July 2015
Published 24 August 2015

Abstract

We propose an accurate tight-binding parametrization for the band structure of MoS_2 monolayers near the main energy gap. We introduce a generic and straightforward derivation for the band energies equations that could be employed for other monolayer dichalcogenides. A parametrization that includes spin–orbit coupling is also provided. The proposed set of model parameters reproduce both the correct orbital compositions and location of valence and conductance band in comparison with *ab initio* calculations. The model gives a suitable starting point for realistic large-scale atomistic electronic transport calculations.

Keywords: MoS2, band structure, tight-binding model, transition metal dichalcogenides

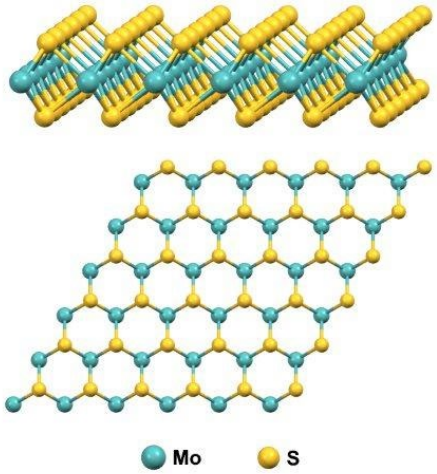

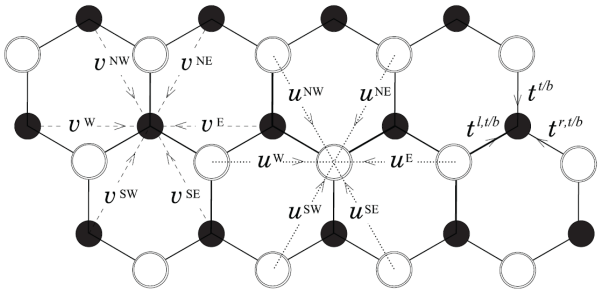

Figure A1. Scheme of the hopping amplitudes. Solid black circles represent Mo atoms, while empty circles represent the S atoms at the top and bottom layers.

Table 6. Tight-binding model parameters obtained by optimization using $a = 3.16$ Å, $\theta_B = 0.710$, and $d = 2.406$ Å.

Parameters	CB–VB optimization (eV)	VB optimization (eV)
D_0	0.201	0.191
D_1	−1.563	−1.599
D_2	−0.352	0.081
D_p	−54.839	−48.934
D_z	−39.275	−37.981
$V_{pd\pi}$	4.196	4.115
$V_{pd\sigma}$	−9.880	−8.963
$V_{pp\sigma}$	12.734	10.707
$V_{pp\pi}$	−2.175	−4.084
$V_{dd\sigma}$	−1.153	−1.154
$V_{dd\pi}$	0.612	0.964
$V_{dd\delta}$	0.086	0.117

Note: The second column gives the best parameter set we obtain to fit both the valence (VB) and the conduction (CB) bands, while the third column focuses the optimization on the valence band.

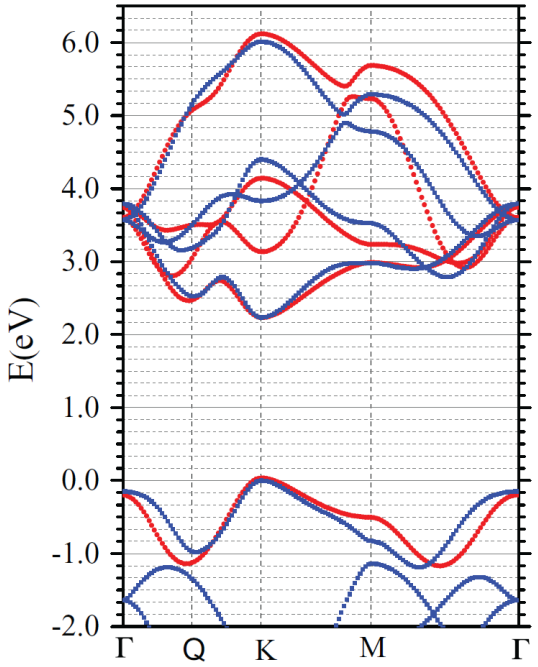

Figure 5. Comparison between the band structures obtained with the DFT-HSE06 (blue squares) and with the optimized tight-binding model using the parameters from the CB–VB optimization (red circles) near the gap region.

Trouble with Simplistic Hamiltonians for Van der Waals Heterostructures

$$\mathbf{v_k} = \frac{1}{\hbar}\frac{\partial \epsilon_\mathbf{k}}{\partial \mathbf{k}} + \frac{d\mathbf{k}}{dt} \times \Omega_\mathbf{k} \Rightarrow \sigma_{xy}^{K,K'} = \frac{e^2}{\pi h}\int d^2k\, f(\varepsilon_\mathbf{k})\Omega_\mathbf{k} \Rightarrow \sigma_{xy}^{v} = \sigma_{xy}^{K} - \sigma_{xy}^{K'} = 2e^2/h$$

Science **346**, 448 (2014)

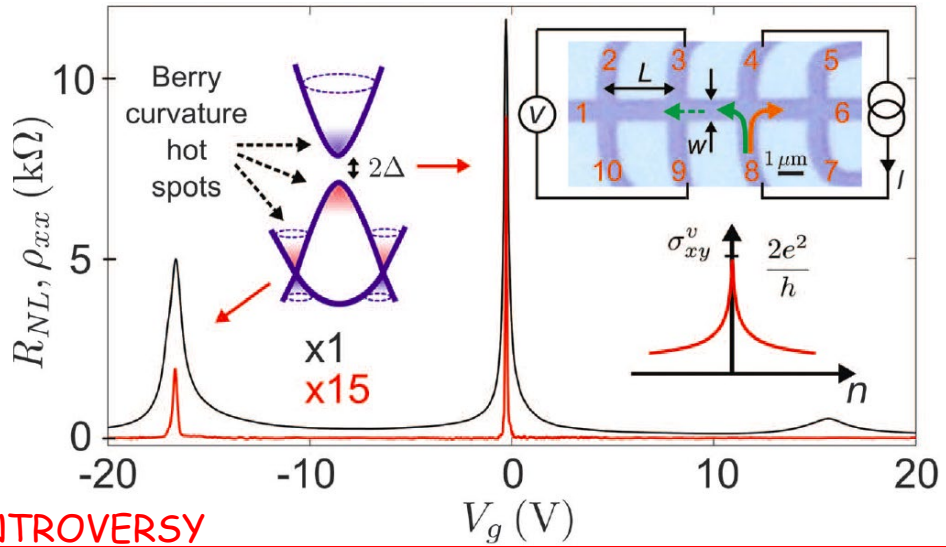

PRB **79**, 035304 (2009)

$$R_{\rm NL} \propto (\sigma_{xy}^{v})^2 \rho_{xx}^3 e^{-L/\ell_v}$$

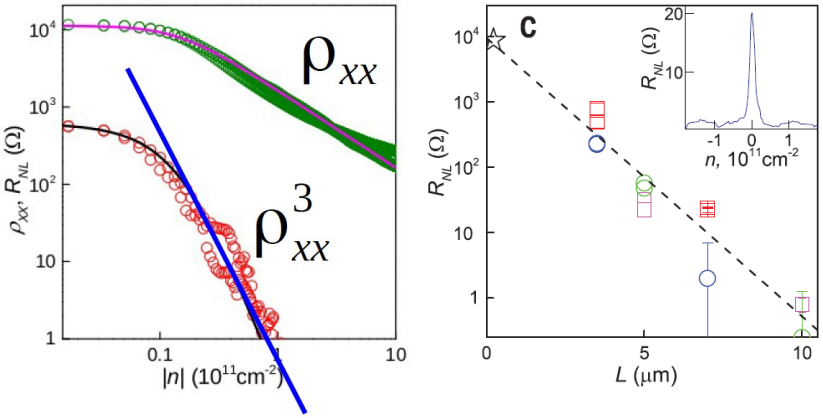

CONTROVERSY

Nat. Commun. **8**, 14552 (2017)

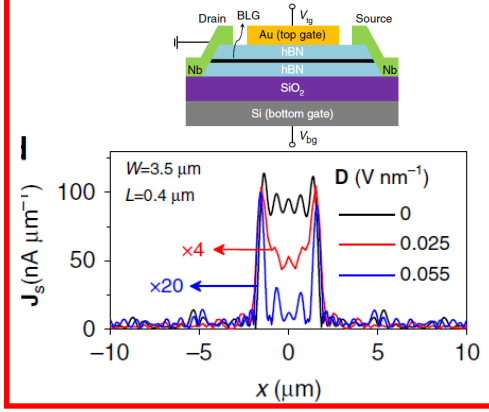

Sci. Adv. **4**, eaaq0194 (2018)

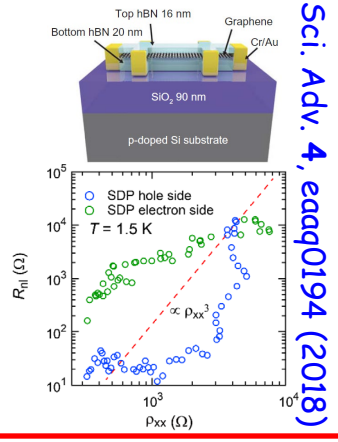

J. Phys. Mater. 1, 0150061 (2018)

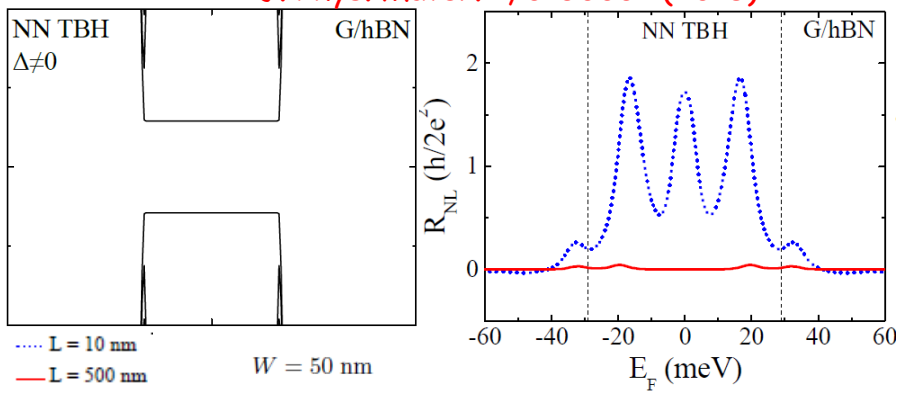

Resolution of the Trouble with *Ab Initio* TBHs

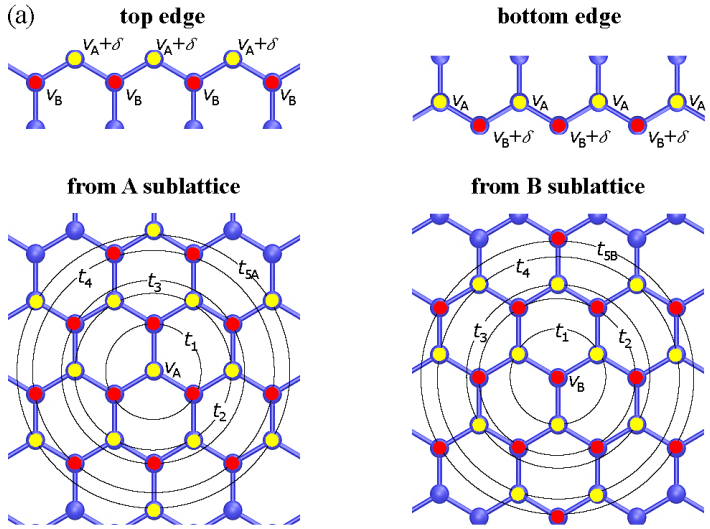

(b)

Isolated graphene wire with zigzag edges	Graphene-on-hBNwire with zigzag edges
$v_A = 0.3667$ eV	$v_A = 0.3495$ eV
$v_B = 0.3667$ eV	$v_B = 0.352$ eV
$\delta = 0.06262$ eV	$\delta = 0.0855$ eV
$t_1 = 2.6672$ eV	$t_1 = 2.6672$ eV
$t_2 = 0.2083$ eV	$t_2 = 0.2083$ eV
$t_3 = 0.2000$ eV	$t_3 = 0.2000$ eV
$t_4 = -0.1800$ eV	$t_4 = -0.1800$ eV
$t_{5A} = 0.0416$ eV	$t_{5A} = 0.0416$ eV
$t_{5B} = 0.0416$ eV	$t_{5B} = 0.0428$ eV

Edge currets for TBH

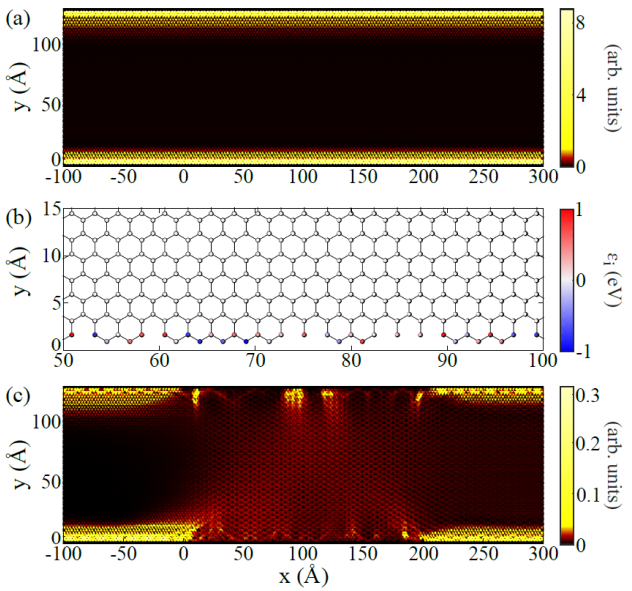

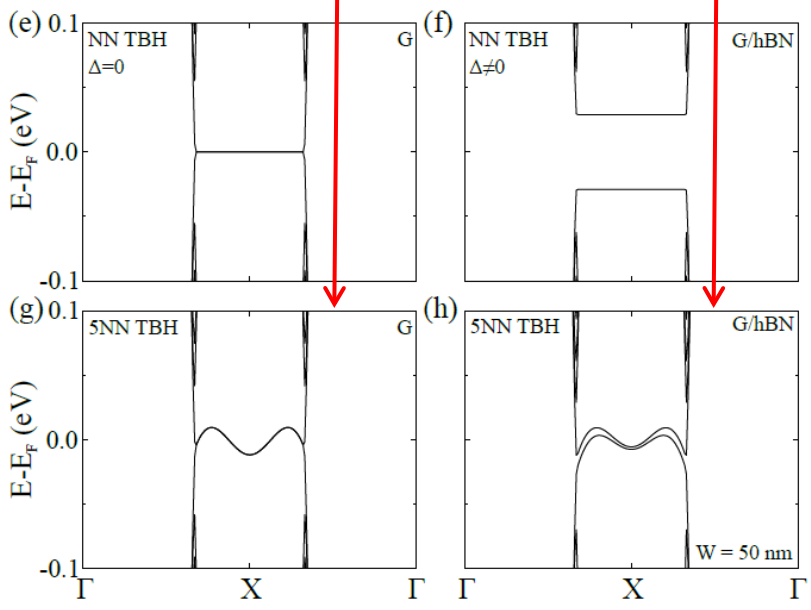

J. Phys. Mater. 1, 015006 1 (2018)

Construction of *Ab Initio* TBH in the basis of Maximally Localized Wannier Functions (MLWF)

RMP **84**, 1419 (2012)

MLWF: Faithfully retain the overlap matrix elements and their phases, the orbital character of the bands and the accuracy of the original DFT calculations, but at the computational cost of TBH

WF — Bloch state

$$w_{n\mathbf{R}}(\mathbf{r}) = \frac{V}{(2\pi)^3}\int_{\mathrm{BZ}} d^3\mathbf{k}\,\Psi_{n\mathbf{k}}(\mathbf{r})e^{-i\mathbf{k}\cdot\mathbf{R}}$$

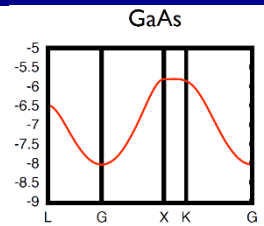

multiband generalized WF (localization in **R** gives Bloch smoothness in **k**)

$$w_{n\mathbf{R}}(\mathbf{r}) = \frac{V}{(2\pi)^3}\int_{\mathrm{BZ}} d^3\mathbf{k}\left[\sum_m U^{\mathbf{k}}_{mn}\Psi_{m\mathbf{k}}(\mathbf{r})\right]e^{-i\mathbf{k}\cdot\mathbf{R}}$$

chosen to minimize quadratic spread

$$\Omega = \sum_n \left[\langle \mathbf{0}n|\hat{r}^2|\mathbf{0}n\rangle - \langle \mathbf{0}n|\hat{\mathbf{r}}|\mathbf{0}n\rangle^2\right]$$

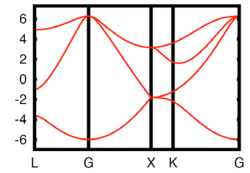

Examples: Graphene and Graphene/hBN

PRB **92**, 205108 (2015)

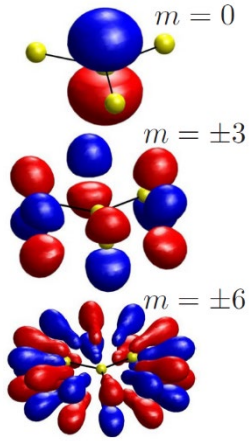

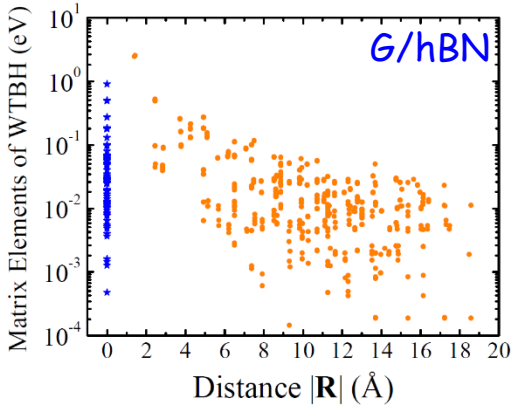

Amplitude isosurface contours of MLWF for graphene is split into the dominant p_z component with m = 0 angular momentum, plus two additional components with m = 3 and m = 6 angular momentum (which is defined up to module 3 due to restoration of threefold rotation symmetry at the position of C atom) whose radius increases with m

Wannier TBH vs. fitted Slater-Koster TBH

arXiv:1508.07735

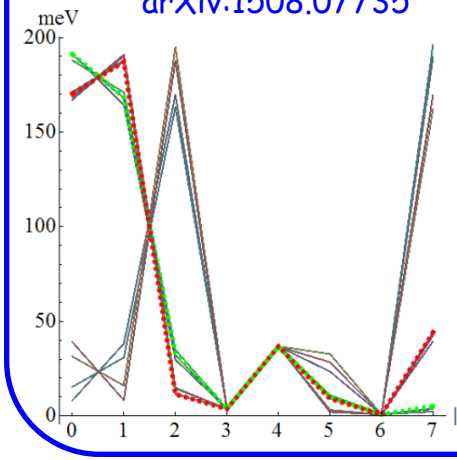

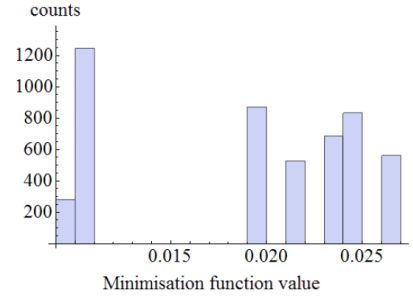

FIG. 6: Instability of fitting with many parameters. 5000 fits of an 8 t tight-binding model to the band structure of $TMTTF_2AsF_6$ produced in [7]. Each line is a set of parameters resulting from one run of the fitting algorithm. The best fit parameters are shown in red. They are inconsistent with the parameters found from Wannier orbital overlaps (given in green). Only 1.5% of the runs found the minimal value of the objective function. The histogram shows the sets of minimisation function values produced in the 5000 runs. Less than 6% of runs are in the 'best' segment of the histogram, and 1/4 in the best two segments.

Beyond DFT: GW and DFT+GW for Weakly-Correlated Systems

$$\hat{H}_0\phi_n^{qp}(\mathbf{r}) + \int d\mathbf{r}'\,\hat{\Sigma}(\mathbf{r},\mathbf{r}';E_n^{qp})\phi_n^{qp}(\mathbf{r}') = E_i^{qp}\phi_n^{qp}(\mathbf{r})$$

H_0 is the (Hermitian) Hamiltonian of a single particle in external potential of ions and classical Hartree potential

$$\hat{\Sigma}(\mathbf{r},\mathbf{r}';\omega) = \frac{i}{4\pi}\int_{-\infty}^{\infty} e^{i\omega'\delta} G(\mathbf{r},\mathbf{r}';\omega+\omega')W(\mathbf{r},\mathbf{r}',\omega')d\omega'$$

Green function

screened Coulomb interaction

The total quasiparticle Hamiltonian is non-Hermitian!

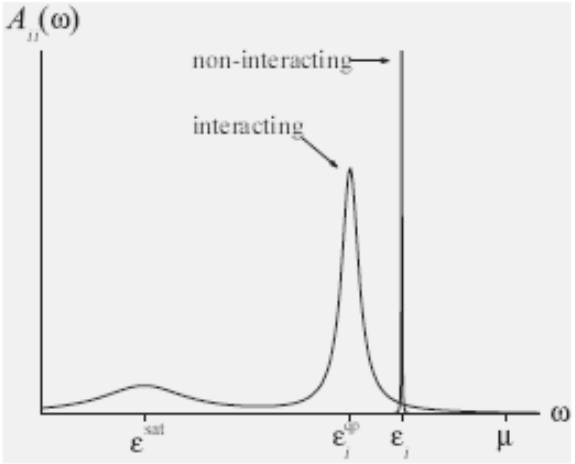

$$E_n^{qp} \simeq \varepsilon_n^{\mathrm{KS}} + \langle\phi_n|\Sigma(\varepsilon_n^{\mathrm{KS}}) - v_{\mathrm{xc}} - \Delta\mu|\phi_n\rangle$$

In many cases there is an almost complete overlap between the QP and the KS wavefunctions, and the full resolution of the QP equation may be circumvented by computing the quasiparticle energy using a first-order perturbation of the KS energy.

- Both hybrid functionals and GW method can lead to semiconductor band gaps in far better agreement with experiment → beyond that, GW also describes quasiparticle renormalizations, finite life times, and improves on the total energies of, e.g., defects

DFT vs. GW Band Structure and LDOS Tested via ARPES on the Surface of Bi_2Te_3

PHYSICAL REVIEW B **90**, 075105 (2014)

Bulk band structure of Bi_2Te_3

Matteo Michiardi,[1] Irene Aguilera,[2] Marco Bianchi,[1] Vagner Eustáquio de Carvalho,[3] Luiz Orlando Ladeira,[3] Nayara Gomes Teixeira,[3] Edmar Avellar Soares,[3] Christoph Friedrich,[2] Stefan Blügel,[2] and Philip Hofmann[1]
[1]*Department of Physics and Astronomy, Interdisciplinary Nanoscience Center, Aarhus University, 8000 Aarhus C, Denmark*
Peter Grünberg Institute and Institute for Advanced Simulation, Forschungszentrum Jülich and JARA, D-52425 Jülich, Germany
[3]*Departamento de Física, ICEx, Universidade Federal de Minas Gerais, 30123-970 Belo Horizonte, MG, Brazil*

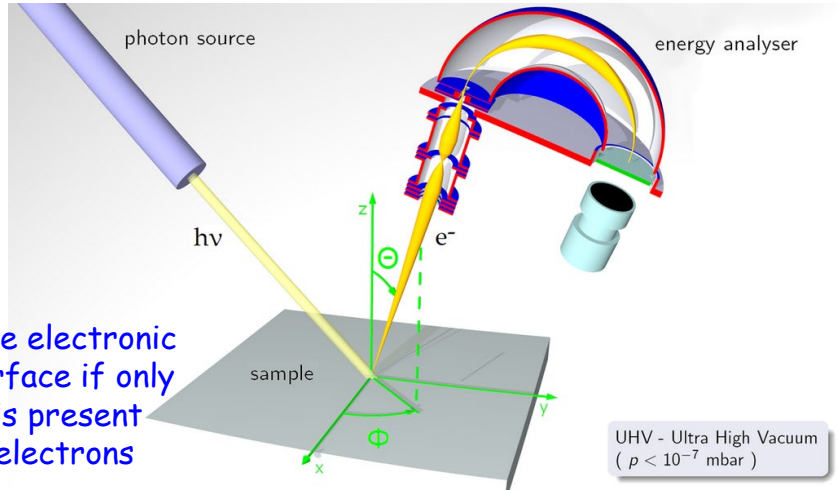

Using moderate energy, ARPES can observe electronic states that are buried deep below the surface if only an evanescent tail of the wave function is present within the mean free path of the photoelectrons

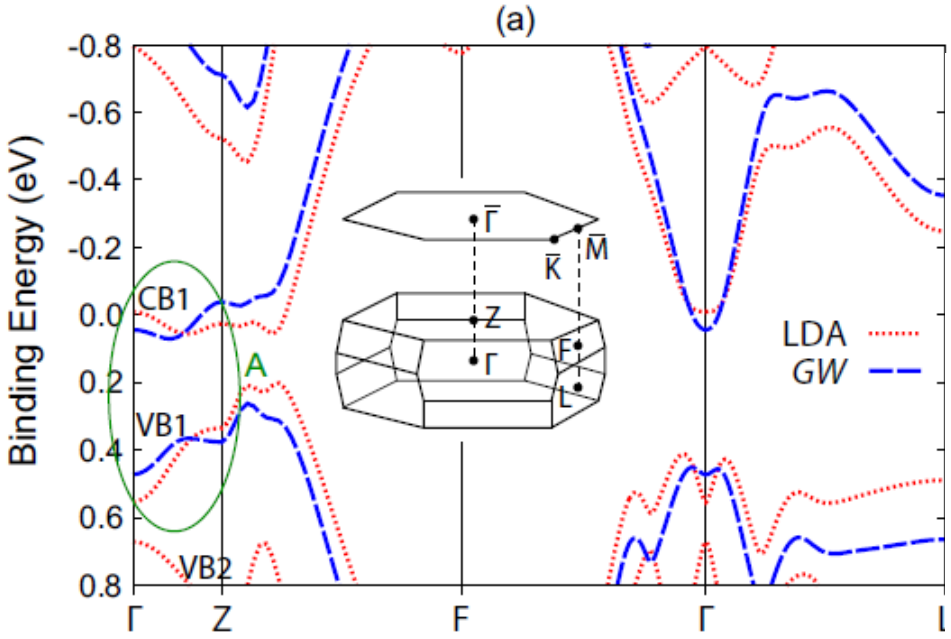

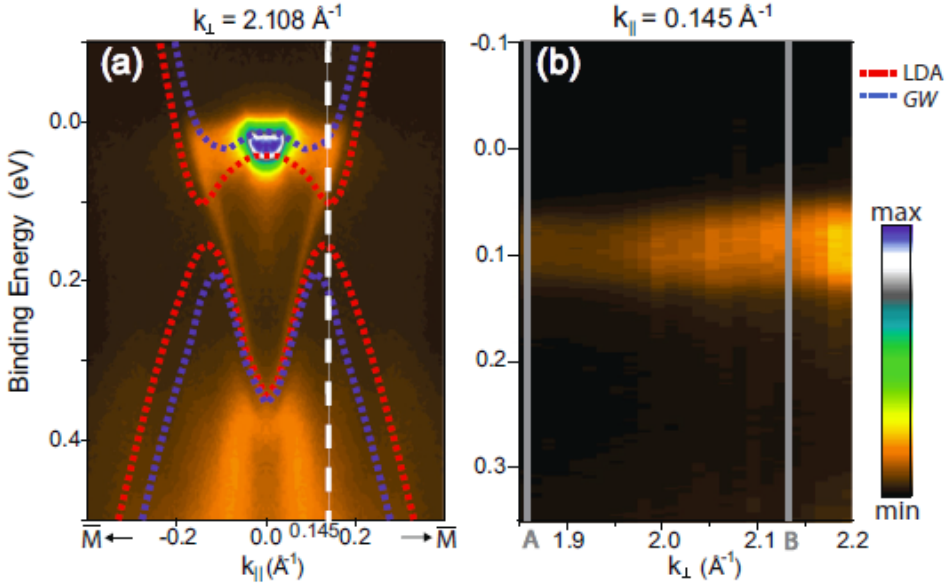

Beyond DFT: DMFT and DFT+DMFT for Strongly Correlated Materials

Advances in Physics,
Vol. 56, No. 6, November–December 2007, 829–926

Taylor & Francis
Taylor & Francis Group

Electronic structure calculations using dynamical mean field theory

K. HELD*

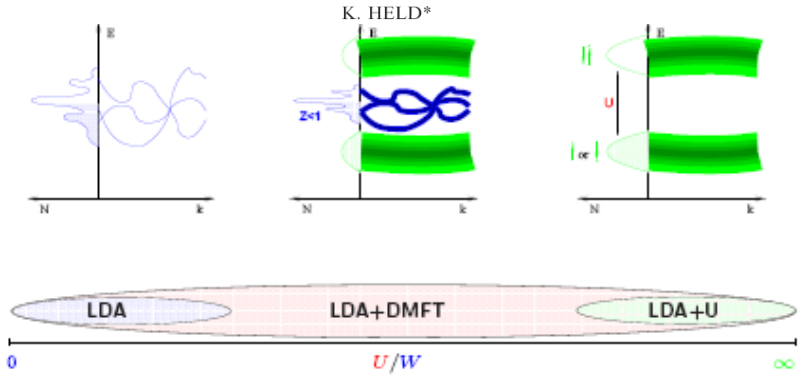

Figure 2.

Weakly correlated metal: The on-site Coulomb interaction is weak compared to the LDA bandwidth: $U \ll W$; and LDA gives the correct answer, typically a (weakly correlated) metal for which we schematically draw a density of states N at energies E and the bandstructure, i.e. E vs. wave vector $\mathbf{k}$.

Strongly correlated metal: In this intermediate regime, one has already Hubbard bands, like for $U/W \gg 1$ (right hand side), but at the same time a remainder of the weakly correlated LDA metal (left hand side), in form of a quasiparticle peak: The $(U=0)$ LDA bandstructure is reproduced, albeit with its width and weight reduced by a factor Z and life time effects which result in a Lorentzian broadening of the quasiparticle levels.

Mott insulator: If the Coulomb interaction U becomes large $(U \gg W)$, the LDA band splits into two Hubbard bands, and we have a Mott insulator with only the lower band occupied (at integer fillings). Such a splitting can be described by the so-called LDA+U method with the drawbacks discussed in the text.

The success of DFT shows that this treatment is actually sufficient for many materials, both for calculating ground state energies and band structures, implying that electronic correlations are rather weak in these materials. But, there are important classes of materials where DFT fails, such as transition metal oxides or heavy fermion systems. In these materials the valence orbitals are partially filled 3d and 4f orbitals. For two electrons in these orbitals the distance is particularly short, and electronic correlations particularly strong.

Many such transition metal oxides are Mott insulators, where the on-site Coulomb repulsion U splits the LDA bands into two sets of Hubbard bands. **One can envisage the lower Hubbard band as consisting of all states with one electron on every lattice site and the upper Hubbard band as those states where two electrons are on the same lattice site.** Since it costs an energy U to have two electrons on the same lattice sites, the latter states are completely empty and the former completely filled with a gap of size U in-between. Other transition metal oxides and heavy fermion systems are strongly correlated metals, with heavy quasiparticles at the Fermi energy, described by an effective mass or inverse weight $m/m_0=1/Z \gg 1$.

Beyond DFT: Coulomb Blockade in Nanostructures

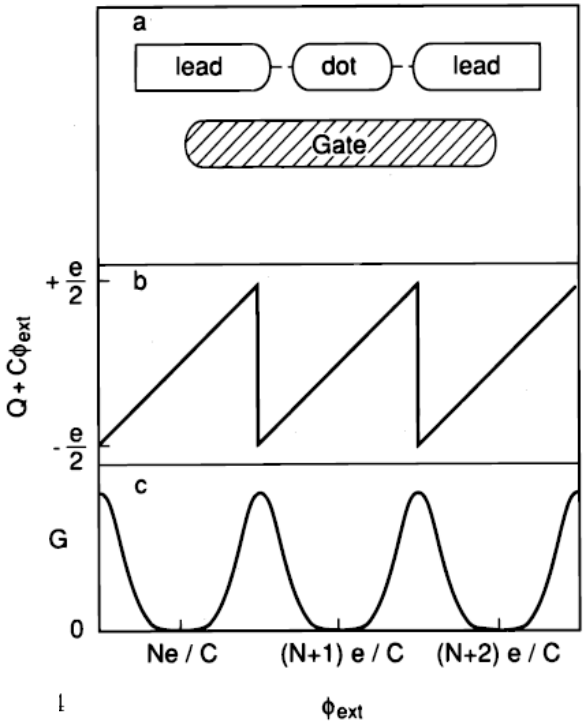

FIG. 1 (a) Schematic illustration of a confined region (dot) which is weakly coupled by tunnel barriers to two leads. (b) Because the charge $Q = -Ne$ on the dot can only change by multiples of the elementary charge e, a charge imbalance $Q + C\phi_{\text{ext}}$ arises between the dot and the leads. This charge imbalance oscillates in a saw-tooth pattern as the electrostatic potential ϕ_{ext} is varied (ϕ_{ext} is proportional to the gate voltage). (c) Tunneling is possible only near the charge-degeneracy points of the saw-tooth, so that the conductance G exhibits oscillations. These are the "Coulomb-blockade oscillations".

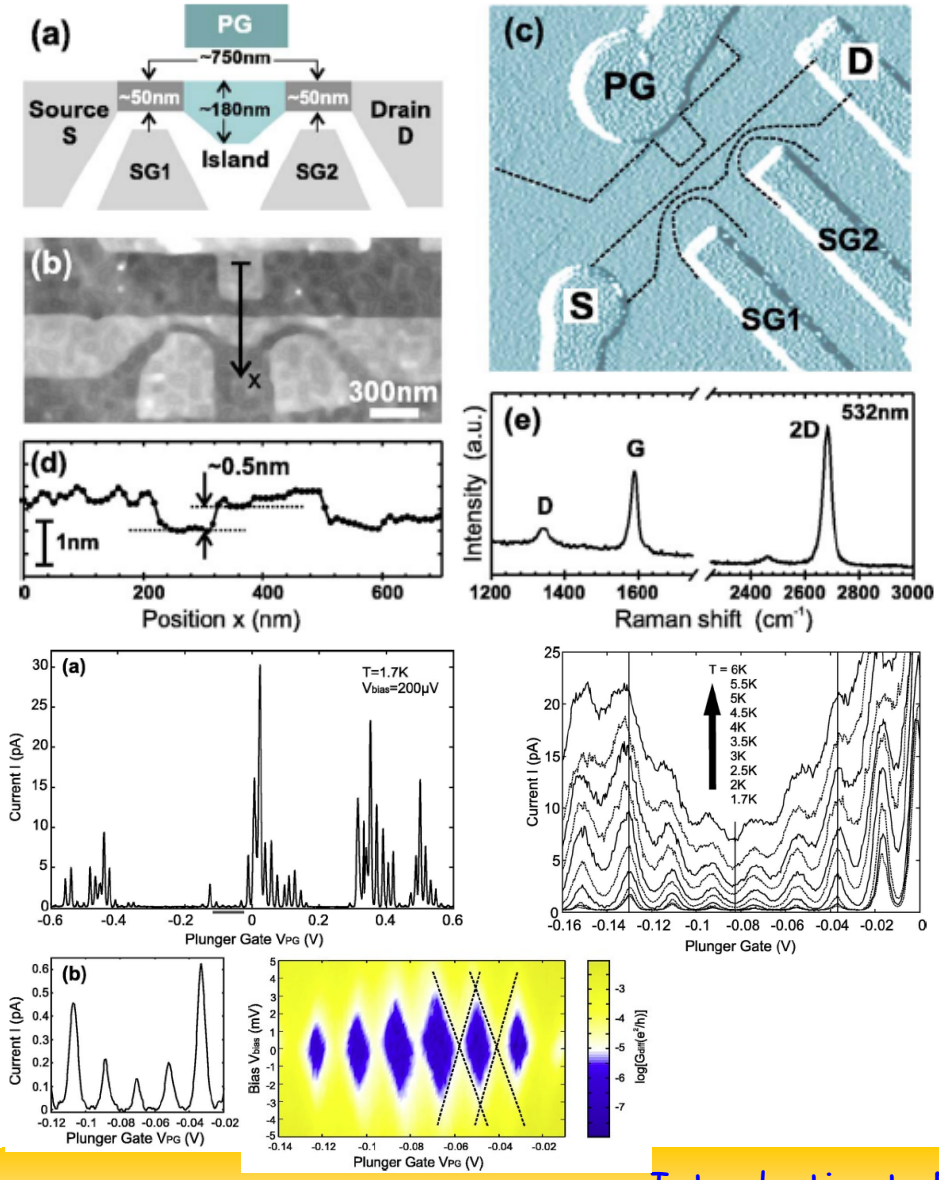

H. van Houten, C. W. J. Beenakker, and A. A. M. Staring, cond-mat/0508454

Ensslin Lab, APL **92**, 012102 (2008)

DFT References for Beginners

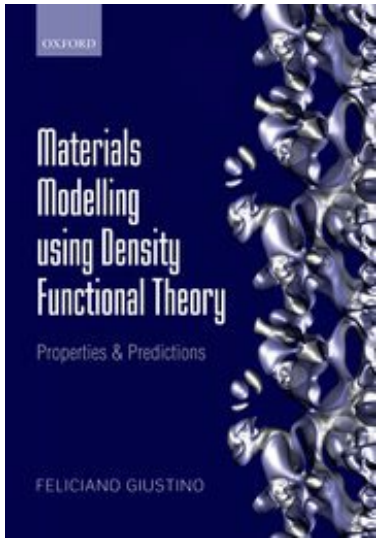

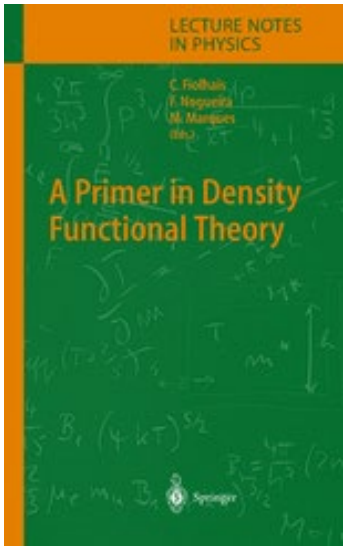

Advances in Physics,
Vol. 56, No. 6, November–December 2007, 829–926

Taylor & Francis
Taylor & Francis Group

Electronic structure calculations using dynamical mean field theory

K. HELD*

Max-Planck-Institut für Festkörperforschung, D-70569 Stuttgart, Germany

(*Received 29 November 2006; in final form 9 August 2007*)

The calculation of the electronic properties of materials is an important task of solid-state theory, albeit particularly difficult if electronic correlations are strong, e.g., in transition metals, their oxides and in *f*-electron systems. The standard approach to material calculations, the density functional theory in its local density approximation (LDA), incorporates electronic correlations only very rudimentarily and fails if the correlations are strong. Encouraged by the success of dynamical mean field theory (DMFT) in dealing with strongly correlated model Hamiltonians, physicists from the bandstructure and the many-body communities have joined forces and developed a combined LDA + DMFT method recently. Depending on the strength of electronic correlations, this new approach yields a weakly correlated metal as in the LDA, a strongly correlated metal or a Mott insulator. This approach is widely regarded as a breakthrough for electronic structure calculations of strongly correlated materials. We review this LDA + DMFT method and also discuss alternative approaches to employ DMFT in electronic structure calculations, e.g., by replacing the LDA part with the so-called GW approximation. Different methods to solve the DMFT equations are introduced with a focus on those that are suitable for realistic calculations with many orbitals. An overview of the successful application of LDA + DMFT to a wide variety of materials, ranging from Pu and Ce, to Fe and Ni, to numerous transition metal oxides, is given.

A bird's-eye view of density-functional theory

Klaus Capelle

(Submitted on 20 Nov 2002 (v1), last revised 18 Nov 2006 (this version, v5))

This paper is the outgrowth of lectures the author gave at the Physics Institute and the Chemistry Institute of the University of Sao Paulo at Sao Carlos, Brazil, and at the VIII'th Summer School on Electronic Structure of the Brazilian Physical Society. It is an attempt to introduce density-functional theory (DFT) in a language accessible for students entering the field or researchers from other fields. It is not meant to be a scholarly review of DFT, but rather an informal guide to its conceptual basis and some recent developments and advances. The Hohenberg-Kohn theorem and the Kohn-Sham equations are discussed in some detail. Approximate density functionals, selected aspects of applications of DFT, and a variety of extensions of standard DFT are also discussed, albeit in less detail. Throughout it is attempted to provide a balanced treatment of aspects that are relevant for chemistry and aspects relevant for physics, but with a strong bias towards conceptual foundations. The paper is intended to be read before (or in parallel with) one of the many excellent more technical reviews available in the literature.